33. Li, X., Zhao, X., Fang, Y., Jiang, X., Duong, T., Fan, C., Huang, C. C. and Kain, S. R. (1998) Generation of destabilized green fluorescent protein as a transcription reporter. J. Biol. Chem. **273**: 34970–34975.
34. Oya, N., Zolzer, F., Werner, F. and Streffer, C. (2003) Effects of serum starvation on radiosensitivity, proliferation and apoptosis in four human tumor cell lines with different p53 status. Strahlenther Onkol. **179**: 99–106.
35. Harada, H., Hiraoka, M. and Kizaka-Kondoh, S. (2002) Antitumor effect of TAT-oxygen-dependent degradation-caspase-3 fusion protein specifically stabilized and activated in hypoxic tumor cells. Cancer Res. **62**: 2013–2018.
36. Heim, R., Prasher, D. C. and Tsien RY. (1994) Wavelength mutations and posttranslational autoxidation of green fluorescent protein. Proc. Natl. Acad. Sci. U S A. **91**:12501–12504.
37. Serganova, I., Doubrovin, M., Vider, J., Ponomarev, V., Soghomonyan, S., Beresten, T., Ageyeva, L., Serganov, A., Cai, S., Balatoni, J., Blasberg, R. and Gelovani, J. (2004) Molecular imaging of temporal dynamics and spatial heterogeneity of hypoxia-inducible factor-1 signal transduction activity in tumors in living mice. Cancer Res. **64**: 6101–6108.
38. Krieg, M., Haas, R., Brauch, H., Acker, T., Flamme, I. and Plate, K. H. (2000) Up-regulation of hypoxia-inducible factors HIF-1alpha and HIF-2alpha under normoxic conditions in renal carcinoma cells by von Hippel-Lindau tumor suppressor gene loss of function. Oncogene. **19**: 5435–5443.
39. Ema, M., Taya, S., Yokotani, N., Sogawa, K., Matsuda, Y. and Fujii-Kuriyama, Y. (1997) A novel bHLH-PAS factor with close sequence similarity to hypoxia-inducible factor 1alpha regulates the VEGF expression and is potentially involved in lung and vascular development. Proc. Natl. Acad. Sci. U S A. **94**: 4273–4278.
40. Yeo, E. J., Chun, Y. S., Cho, Y. S., Kim, J., Lee, J. C., Kim, M. S. and Park, J. W. (2003) YC-1: a potential anticancer drug targeting hypoxia-inducible factor 1. J. Natl. Cancer Inst. **95**: 516–525.
41. Inoue, M., Mukai, M., Hamanaka, Y., Tatsuta, M., Hiraoka, M. and Kizaka-Kondoh, S. (2004) Targeting hypoxic cancer cells with a protein prodrug is effective in experimental malignant ascites. Int. J. Oncol. **25**: 713–720.

Received on November 19, 2004
1st Revision received on December 22, 2004
Accepted on December 22, 2004

Optical Imaging of Tumor Hypoxia and Evaluation of Efficacy of a Hypoxia-Targeting Drug in Living Animals

Hiroshi Harada, Shinae Kizaka-Kondoh, and Masahiro Hiraoka

Kyoto University Graduate School of Medicine, Japan

Abstract

Solid tumors containing more hypoxic regions show a more malignant phenotype by increasing the expression of genes encoding angiogenic and metastatic factors. Hypoxia-inducible factor-1 (HIF-1) is a master transcriptional activator of such genes, and thus, imaging and targeting hypoxic tumor cells where HIF-1 is active are important in cancer therapy. In the present study, HIF-1 activity was monitored via an optical in vivo imaging system by using a luciferase reporter gene under the regulation of an artificial HIF-1-dependent promoter, 5HRE. To monitor tumor hypoxia, we isolated a stable reporter-transfectant, HeLa/5HRE-Luc, which expressed more than 100-fold luciferase in response to hypoxic stress, and observed bioluminescence from its xenografts. Immunohistochemical analysis of the xenografts with a hypoxia marker, pimonidazole, confirmed that the luciferase-expressing cells were hypoxic. Evaluation of the efficacy of a hypoxia-targeting prodrug, TOP3, using this optical imaging system revealed that hypoxic cells were significantly diminished by TOP3 treatment. Immunohistochemical analysis of the TOP3-treated xenografts confirmed that hypoxic cells underwent apoptosis and were removed after TOP3 treatment. These results demonstrate that this model system using the 5HRE-luciferase reporter construct provides qualitative information (hypoxic status) of solid tumors and enables one to conveniently evaluate the efficacy of cancer therapy on hypoxia in malignant solid tumors. *Mol Imaging* (2005) **4**, 182–193.

Keywords: Hypoxia-inducible factor-1 (HIF-1), tumor hypoxia, hypoxia response element (HRE), luciferase bioluminescence, optical imaging.

Introduction

An insufficient blood supply to a rapidly growing tumor leads to the presence of hypoxia, which is a well-known feature of solid tumors [1]. It is clinically important that insufficient tumor oxygenation affects the efficiency of chemotherapy and radiotherapy [2–4]. Moreover, hypoxic conditions increase the aggressiveness of tumor cells by inducing the expression of several genes related to proliferation, angiogenesis, invasion, and metastasis to aid survival in the severe tumor microenvironment [5–7]. Most of such genes contain a hypoxia responsive element (HRE), which is the binding site of hypoxia inducible factor-1 (HIF-1) [8], the master transcriptional regulator of cellular adaptive responses to hypoxic stress [5,9]. HIF-1 is a heterodimer that consists of an alpha subunit (HIF-1α) and the constitutively expressed beta subunit (HIF-1β). HIF-1α expression is regulated in an oxygen-dependent manner at the posttranslational level and is responsible for the regulation of HIF-1 activity [9]. In normoxia, HIF-1α is hydroxylated on the proline residues in the oxygen-dependent degradation domain (ODD) by prolyl hydroxylases [10,11]. The hydroxylated proline residues accelerate the interaction of HIF-1α protein with von Hippel–Lindau tumor suppressor protein, resulting in the rapid ubiquitination and subsequent degradation of HIF-1α [5,12–15].

HIF-1 as well as tumor hypoxia have been recognized as a crucial target for cancer therapy, therefore, strategies detecting and evaluating them are desired [5,16]. Recently, hypoxia-responsive promoters have been applied to develop hypoxia imaging and targeting strategies. HRE derived from vascular endothelial cell growth factor (VEGF) promoter [8] has been employed to establish the artificial hypoxia-responsive promoter. The promoters containing HRE in tandem significantly increase the gene expressions in response to hypoxic stress and successfully induce anti-tumor effects in vivo [17–22]. Above all, 5HRE promoter, which consists of five copies of HRE and human cytomegalovirus minimal promoter, enhances more than 500-fold transcription under the hypoxic conditions than under the aerobic conditions [19]. Green fluorescent protein [20,21] and a prodrug-activating enzyme [22] under the regulation of 5HRE promoter show the potential for tumor hypoxia-specific imaging and targeting, respectively. We have

Abbreviations: HE, hematoxylin–eosin; HIF, hypoxia-inducible factor; HIV-1, human immunodeficiency virus type-1; HRE, hypoxia response element; ODD, oxygen-dependent degradation; PTD, protein transduction domain; siRNA, small interfering RNA; TOP3, tat-ODD-procaspase-3; TUNEL, TdT-mediated dUTP nick end labelling; VEGF, vascular endothelial growth factor.

Corresponding author: Shinae Kizaka-Kondoh, COE Formation for Genomic Analysis of Disease Model Animals with Multiple Genetic Alterations, Department of Radiation Oncology and Imaging-applied Therapy, Kyoto University Graduate School of Medicine, 54 Kawahara-cho, Shogoin, Sakyo-ku, Kyoto, 606-8507, Japan; e-mail: skondoh@kuhp.kyoto-u.ac.jp.

Received 31 January 2005; Received in revised form 24 March 2005; Accepted 3 May 2005.

developed a protein prodrug, TOP3 [23,24], which is composed of the protein transduction domain derived from human immunodeficiency virus-1 tat protein (HIV tat-PTD), a part of HIF-1α ODD domain and the dormant form of caspase-3, procaspase-3. HIV tat-PTD fusion proteins can be delivered to many different cells in the whole body in a concentration-dependent manner [25,26] and ODD fusion proteins can be specifically stabilized under hypoxic conditions [23]. Therefore, hypoxia-specific targeting of tumor cells has been accomplished by TOP3 in hypoxic ascites as well as in vitro [23,27].

In this report, we demonstrate that the imaging system using a 5HRE-luciferase reporter gene can efficiently detect and monitor tumor hypoxia where HIF-1 is active in living mice. By using this system, we successfully demonstrate that TOP3 certainly targets hypoxic tumor cells in solid tumors, indicating that this model system allows sensitive, real-time, and spatio-temporal analyses of tumor hypoxia in solid tumors and provides a useful method to evaluate the efficacy of a cancer therapy on hypoxia in malignant solid tumors.

Materials and Methods

Cell Cultures, Reagents, and Hypoxic Treatment

The human cervical epithelial adenocarcinoma cell line, HeLa, and the human pancreatic cancer cell line, CFPAC-1, were purchased from the American Type Culture Collection (#CCL-2 and #CRL-1918, respectively). HeLa cells were maintained in 5% FBS–Dulbecco's modified Eagle's medium, and CFPAC-1 cells were maintained in 10% FBS–Iscove's modified Dulbecco's medium (Nacalai Tesque, Kyoto, Japan). Both of the mediums were supplemented with penicillin (100 units/mL) and streptomycin (100 μg/mL). To create a hypoxic condition of <0.02% of oxygen tension, the cells were treated in a Bactron Anaerobic Chamber, BACLITE-1 (Sheldon Manufacturing, Cornelius, OR).

Preparation of Protein Prodrug

TOP3 was overexpressed in *Escherichia coli* and purified as described previously [23]. Purified TOP3 was dissolved in Tris–HCl buffer (pH 8.0) at a concentration of 1 mg/mL.

Plasmid DNA

To construct the pEF/Luc plasmid, which constitutively expresses luciferase under the control of EF-1α promoter [28], luciferase cDNA was amplified from pGL3 promoter vector (Promega, Madison, WI) by PCR using Luc-Bam-sense primer; AAGGATCCACCATGGAAGACGCCAAA and Luc-RV-anti primer; TTGATATCTTACACGGCGATCTTTCC. The PCR product was then digested with *Bam*HI and *Eco*RV and inserted between *Bam*HI and *Eco*RV recognition sites of pEF6/Myc-His B plasmid (Invitrogen, Carlsbad, CA). To construct the pEF/5HRE-Luc plasmid, the DNA fragment, which consists of 5HRE promoter and luciferase gene, was obtained by *Kpn*I and *Xba*I digestion of 5HRE-hCMVmp-Luc plasmid [19] and inserted between *Kpn*I and *Xba*I recognition sites of pEF/myc/cyto plasmid (Invitrogen).

Isolation of HeLa/EF-Luc and HeLa/5HRE-Luc Cells

To establish HeLa/EF-Luc and HeLa/5HRE-Luc cell clones, HeLa cells were transfected with pEF/Luc plasmid and pEF/5HRE-Luc plasmid, respectively, by calcium phosphate method using the Mammalian Transfection Kit (Stratagene, La Jolla, CA) and were selected by culturing for an additional 10 days in the culture medium containing 5 μg/mL of blasticidine S (Invitrogen) for HeLa/EF-Luc or 400 μg/mL of G418 (Nacalai Tesque) for HeLa/5HRE-Luc. Antibiotics-resistant colonies were isolated and established as clones. Representative clones were used here.

Luciferase Assay in vitro and Western Blot Analysis

HeLa/5HRE-Luc cells were seeded onto a 24-well dish (1×10^4 cells/well) and cultured under aerobic or hypoxic conditions for 0, 1, 2, 4, 8, and 16 hr. The cells were then washed with PBS and lyzed with 100 μL Passive Lysis Buffer (Promega) and 10 μL of the lysates were applied for the luciferase assay (Promega). For Western blot analysis, the cells were directly harvested in the 100 μL of 1× loading buffer [29] after the same hypoxic treatment as above, and 20 μL of them were electrophoresed on a 7.5% SDS–polyacrylamide gel and transferred onto PVDF membrane (Amersham Biosciences, Piscataway, NJ). HIF-1α protein was detected with monoclonal anti-HIF-1α antibody (BD Bioscience Pharmingen, San Diego, CA) and anti-mouse IgG horseradish peroxidase linked whole antibody (Amersham Bioscience) using the ECL-PLUS system (Amersham Bioscience) according to the manufacturer's instruction.

Real-time Monitoring of Luciferase Activity in vivo

Cell suspensions of HeLa/EF-Luc cells and HeLa/5HRE-Luc cells (1×10^6 cells/100 μL of PBS) were subcutaneously inoculated into the left and right hind legs of 6-week-old female nude mice (BALB/c *nu/nu*; Japan SLC, Hamamatsu, Japan), respectively. The mice were

used for each experiment 10 days after the implantation. For the in vivo imaging of bioluminescence, the tumor-bearing mice were intravenously injected with 100 μL of D-luciferin solution (10 mg/mL in PBS; Promega). And exactly 15 min later, the mice were applied to IVIS®-100 in vivo Imaging System (Xenogen, Alameda, CA) to measure the luciferase activity as the externally detected photon count. During imaging, the mice were kept on the imaging stage in the anesthetized condition with 2.5% of isoflurane gas in oxygen flow (1.5 L/min). Obtained images were analyzed by using Living Image 2.50—Igor Pro 4.09A software (Xenogen). Pixel intensities within the regions of interest were summed to yield integrated intensity of bioluminescence as photon counts. In all of the imaging experiments, reproducibility was confirmed by using 5 independent tumor-bearing mice, and representative images are shown.

Growth Delay Assay

The tumor mass of CFPAC-1 xenografts was measured with a caliper, and the tumor mass was calculated as $0.5 \times L \times W^2$. The tumor mass of HeLa/EF-Luc xenografts was measured as the externally detected photon counts. The tumor mass on each day was compared with the one on Day 0, to calculate the relative tumor mass.

Immunohistochemical Analysis

Pimonidazole hydrochloride (Natural Pharmacia International, Belmont, MA) was intraperitoneally injected into tumor-bearing mice (60 mg/kg) at 90 min before surgical excision of solid tumor in each experiment. The excised solid tumors were fixed in 10% formalin neutral buffer solution (pH = 7.4; Wako Pure Chemical Industries, Osaka, Japan) and embedded in paraffin.

To detect pimonidazole-binding and luciferase proteins, paraffin-embedded sections were treated with anti-pimonidazole (Natural Pharmacia International) and anti-luciferase (Promega) antibodies, respectively, and stained by indirect immunoperoxidase detection method (DakoCytomation, Carpinteria, CA). Counterstaining with hematoxylin was also conducted. Paraffin-embedded serial sections were also stained with hematoxylin–eosin (HE). To calculate the percentage of hypoxic regions, pimonidazole-positive areas were quantified using NIH Image 1.63 software (NIH, Bethesda, MD) and compared with the one of whole tumor. This analysis was conducted in a double-blind fashion.

For the detection of apoptotic cells, the paraffin-embedded sections were stained with ApopTag Fluorescein In Situ Apoptosis Detection Kit (Chemicon International, Temecula, CA), according to the manufacturer's instruction.

Statistical Analysis

Data are expressed as means ± *SD*. Statistical significance of differences was determined by the paired two-tailed Student's *t* test. Differences were considered statistically significant for $p < .05$.

Results

HIF-1-dependent Luciferase Activity in HeLa/5HRE-Luc Cells

To assess the HIF-1 activity in solid tumors, we took advantage of the HIF-1-mediated gene expression. We isolated a stable HeLa clone (HeLa/5HRE-Luc) after transfection with 5HRE-hCMVmp-Luciferase reporter gene [19], which was reported to induce luciferase expression in response to hypoxic stress. When HeLa/5HRE-Luc cells were cultured under hypoxic conditions, their luciferase activity was increased 100-fold more than the one cultured under aerobic conditions (Figure 1A). HIF-1α proteins were gradually stabilized over the hypoxic treatment periods (Figure 1B). These data indicate

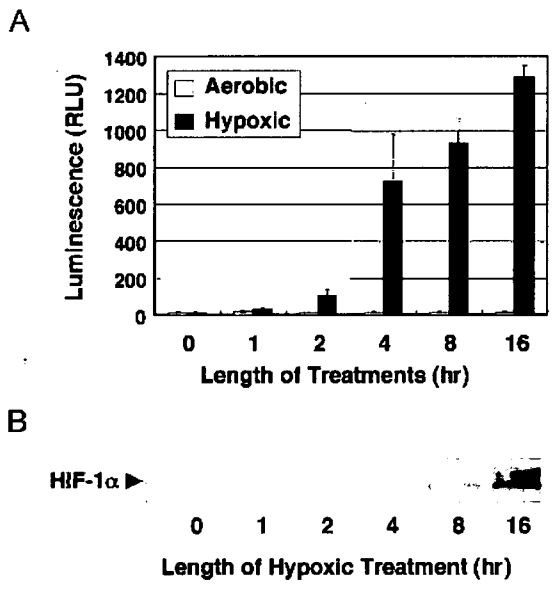

Figure 1. *HIF-1-dependent luciferase activity in HeLa/5HRE-Luc cells. (A) HeLa/5HRE-Luc cells were treated under aerobic or hypoxic conditions for the indicated time and their luciferase activities were measured and luminescence (RLU) is shown in the figure. The results are the mean ± SD, n = 3. (B) HeLa/5HRE-Luc cells were treated under hypoxic conditions for the indicated time and HIF-1α protein expression was analyzed by Western blotting.*

that the HeLa/5HRE-Luc cells can be employed to monitor the oxygen-dependent HIF-1 activity.

Optical Imaging of HIF-1 Activity in Tumor Xenograft

Optical in vivo imaging systems enable us to detect tumor cells in the same animals repeatedly [30], and thus, we can monitor the change of luciferase activity in the same tumor xenografts by measuring bioluminescence throughout the experiment period. We first examined HeLa/5HRE-Luc xenografts by immunohistochemical analysis if luciferase expression was corresponding with hypoxic microenvironment in them. The presence of hypoxic cells in solid tumors was assessed by using a bioreductive hypoxia marker, pimonidazole hydrochloride [31]. The regions detected with anti-luciferase antibody (Figure 2Aa; dark brown) were almost identical to the pimonidazole-positive regions (Figure 2Ab; dark brown), and both were located at the boundary areas between viable (Figure 2Ac; V) and necrotic regions (Figure 2Ac; N), indicating that the cells expressing luciferase were certainly hypoxic. The bioluminescence from the HeLa/5HRE-Luc tumor xenografts was externally monitored by optical in vivo imaging system (Figure 2Ba; right hind leg).

To confirm that the intensity of bioluminescence from HeLa/5HRE-Luc xenografts reflects hypoxic status in the xenografts, we reduced the blood flow to the HeLa/5HRE-Luc xenografts by ligaturing the tumor-bearing right legs and examined the xenografts via an optical in vivo imaging system at the indicated time (Figure 2Ba–Bd). HeLa/EF-Luc tumor xenografts, in which luciferase was constitutively expressed, were set in the left hind legs and were untreated during the experiment as an internal control for the imaging procedure. The bioluminescence from the ligatured HeLa/5HRE-Luc xenografts increased over time (Figure 2Ba–Bd), whereas changes in bioluminescent intensity were hardly observed without ligature (Figure 2Be–Bh). To examine whether the increase in bioluminescence was dependent on the 5HRE promoter, we conducted same experiments using the mice with HeLa/EF-Luc xenografts in both legs. The bioluminescence intensity from the HeLa/EF-Luc xenografts was not influenced by the ligaturing (data not shown). Each experiment was conducted by using 5 independent tumor-bearing mice to confirm reproducibility, and representative images are shown in the figure. These results indicate that the increase of bioluminescence from ligatured HeLa/5HRE-Luc xenograft reflected the increase of hypoxic regions because of poor blood supply and suggest that the 5HRE-luciferase reporter system can be used to monitor tumor hypoxia in solid tumors via in vivo imaging system.

Evaluation of Hypoxia-targeting Efficacy of TOP3 with the Optical Imaging Method

We recently developed an anti-tumor protein prodrug, TOP3, which is composed of HIV-1 tat-PTD, a part of HIF-1α ODD domain and procaspase-3 (Figure 3). Because Tat-PTD ensures the in vivo delivery of fusion protein into a variety of different cells in a rapid and concentration-dependent manner [25,26], and the ODD domain facilitates the specific stabilization of fusion protein under hypoxic conditions [23], tat-ODD fusion protein, whose stability is regulated through the same ODD-dependent mechanism as HIF-1α protein, is accumulated in the hypoxic tumor cells in vivo [23,27]. Accumulated TOP3 is subsequently cleaved by endogenous caspases, which are activated to some extent by hypoxic stress, and increases active caspase-3, resulting in hypoxia-specific cell death in hypoxic ascites as well as in vitro [23,27]. Although TOP3 did reduce the volume of solid tumors, it was not clear if TOP3 targeted hypoxic tumor cells in solid tumors. By using this imaging method, we can monitor hypoxic tumor cells over TOP3 treatment period, and thus, we can clarify the TOP3 effect on solid tumors.

TOP3 was intraperitoneally injected into nude mice (n = 5) with a HeLa/5HRE-Luc xenograft in the right hind leg and with a HeLa/EF-Luc xenograft in the left hind leg three times in 5-day intervals. The bioluminescent signals from both xenografts were monitored via the in vivo imaging system and relative photon counts and representative images are shown (Figure 4A–C). Because the photon count corresponds to tumor mass when the luciferase is constitutively expressed in the tumor cells [30], the effect of TOP3 on whole tumor mass was measured as the bioluminescence from the HeLa/EF-Luc xenograft in the left hind leg. On the other hand, the effect of TOP3 on hypoxic tumor cells was assessed as the bioluminescence from the HeLa/5HRE-Luc xenograft in the right hind leg. The bioluminescent signals from both HeLa/EF-Luc and HeLa/5HRE-Luc xenografts of buffer-treated mice increased over the observation periods (Figure 4A, B, and Ca–Cc). In the buffer-treated mice, the increase in the bioluminescence from hypoxic regions was more than 22-fold (Figure 4B) during the period, in which the whole tumor mass increased about 16-fold (Figure 4A), indicating that hypoxic regions gradually increased as the tumor volume increased. On the other hand, the bioluminescence from hypoxic regions of the TOP3-treated mice was

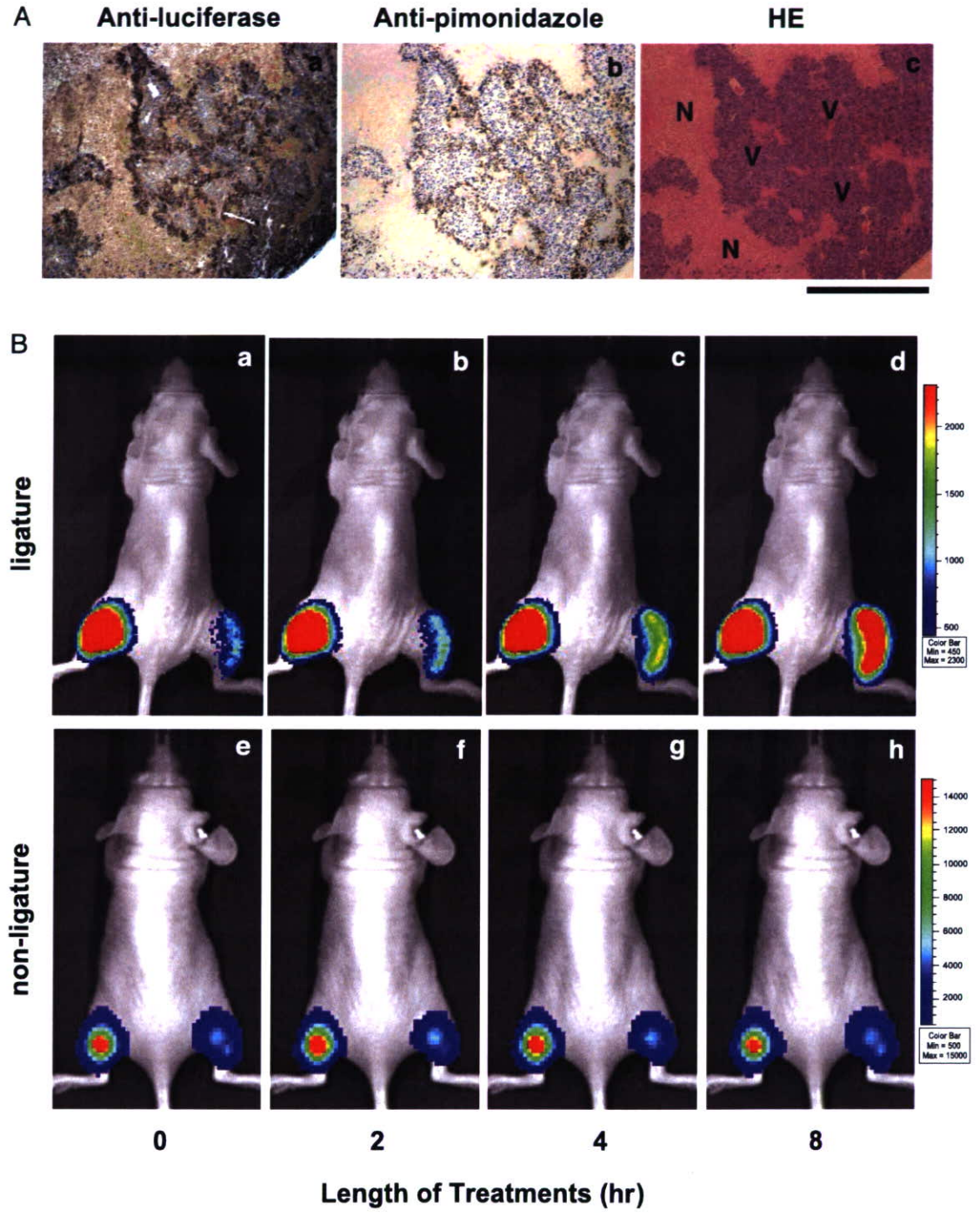

Figure 2. *Optical imaging of HIF-1 activity in HeLa/5HRE-Luc tumor xenografts. (A) Serial sections of HeLa/5HRE-Luc xenograft were subjected to immunohistochemical analysis with anti-luciferase antibody (a) and anti-pimonidazole antibody (b), and to HE staining (c). N = necrotic tumor tissue; V = well-oxygenated viable tumor tissue. (B) HeLa/EF-Luc cells and HeLa/5HRE-Luc cells were subcutaneously inoculated into the left and right hind legs, respectively (a–h). Blood flow to the HeLa/5HRE-Luc xenograft was decreased by ligaturing the right hind leg (a–d). During the ligaturing treatment, change in bioluminescence was sequentially monitored in the same mouse just after (a), 2 hours after (b), 4 hours after (c), and 8 hours after (d) the beginning of ligaturing. As a control, the bioluminescence was sequentially monitored without the ligature at the same time course (e–h). HeLa/EF-Luc xenograft in the left leg was left untreated as an internal control. During the experiment, mice were kept exposed to anesthesia with 2.5% of isoflurane gas in oxygen flow (1.5 L/min) and put on the imaging stage.*

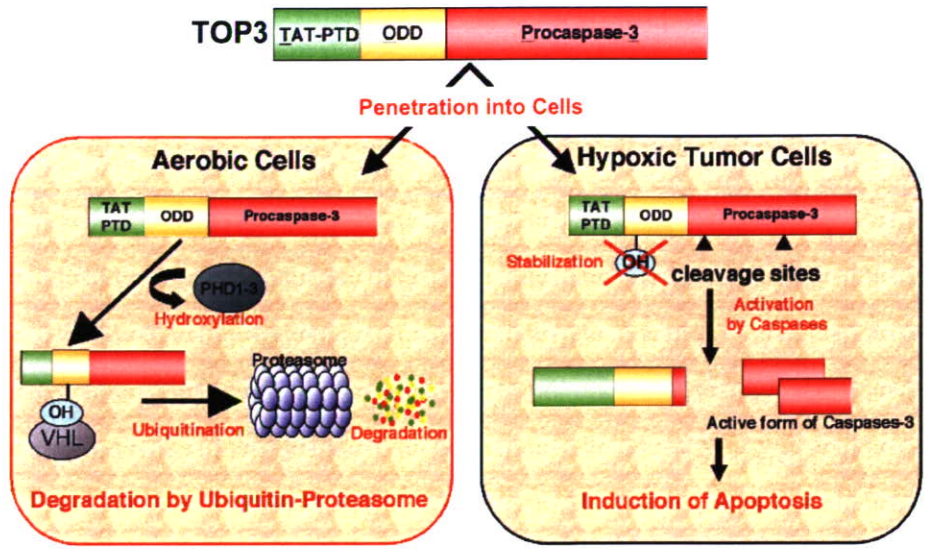

Figure 3. *Oxygen-dependent degradation and hypoxia-specific activation of TOP3. In well-oxygenated cells, TOP3 will be degraded through the same ubiquitin–proteasome system as HIF-1α protein (for details, see Ref. [16]). In hypoxic tumor cells, TOP3 are stabilized, and upstream caspases are activated to some extent by hypoxic stress, and therefore, TOP3 will be cleaved to generate an active caspase-3, inducing apoptotic cell death.*

minimized on Day 3 after the first administration and was continuously suppressed during the treatment period (Figure 4B and Cd–Cf: right legs), in which whole tumor mass increased about 9-fold (Figure 4A). These data clearly demonstrate the hypoxia-targeting effect of TOP3 in solid tumors.

Specific Targeting of Hypoxic Tumor Cells by TOP3 in vivo

To investigate whether the suppressed bioluminescence in TOP3-treated xenografts were the consequence of the reduction of hypoxic/HIF-1-activating cells in solid tumors, we investigated the sections of TOP3-treated xenografts by immunohistochemical analysis. To avoid the influence of luciferase expression, CFPAC-1 xenografts were examined with the same experimental time frame as HeLa/5HRE-Luc xenografts. First of all, we confirmed that the growth of CFPAC-1 xenografts was comparatively suppressed during TOP3 treatment (Figure 5A). The growth of TOP3-treated tumors was suppressed during the sequential TOP3 treatment, but accelerated thereafter (>Day 15); the slope of the growth curve of buffer-treated tumors was 0.211. The slope of the TOP3-treated tumor (from Day 0 to Day 15) was 0.087, but it reverted to a similar slope to that of the untreated tumor after Day 15 (0.225). Tumor growth doubling time (TGDT) clearly shows a growth delay of TOP3-treated tumors (Table 1; $p < .05$). TOP3 treatment decreased the growing speed of the CFPAC-1 tumor to almost one-third of the untreated ones.

The tumors were surgically excised 5, 24, and 48 hr after TOP3 administration, and were embedded in paraffin for HE staining and for immunohistochemical analysis with anti-pimonidazole antibody. We repeated the above staining with three to four independent tumors for each group. The percentage of pimonidazole-positive cells (dark brown) in a whole solid tumor represents the percentage of hypoxic regions (Figure 5B). Hypoxic regions in the 48-hr samples from TOP3-treated xenografts were significantly reduced compared with the ones in buffer-treated xenografts ($p < .01$). The staining pattern of serial sections from the 5-hr samples was basically the same between TOP3-treated and buffer-treated xenografts, whereas the patterns of 24- and 48-hr samples from TOP3-treated xenografts

Figure 4. *Evaluation of the efficacy of TOP3 via an optical in vivo imaging system. Tumor-bearing mice with HeLa/EF-Luc cells (left hind leg) and HeLa/5HRE-Luc cells (right hind leg) were intraperitoneally injected with Tris–HCl buffer (pH 8.0) or TOP3 (20 mg/kg) on Days 0, 5, and 10. (A) To calculate the relative tumor mass during the buffer or TOP3 treatments, the bioluminescence (photons/sec/ROI) from HeLa/EF-Luc tumor xenograft in the left hind leg on each day was divided by the one on Day 0 and shown as relative photon counts. The results are the mean of 5 independent tumor-bearing mice ± SD for each group. *$p < .05$. (B) To calculate the relative hypoxic regions during the buffer or TOP3 treatments, the bioluminescence (photons/sec/ROI) from HeLa/5HRE-Luc tumor xenograft in the right leg on each day was divided by the one on Day 0 and shown as relative photon counts. The results are the mean of 5 independent tumor-bearing mice ± SD for each group. *$p < .05$. **$p < .01$. (C) The bioluminescence was externally monitored by IVIS imaging system to analyze the effects of the TOP3 treatments on the whole tumor mass (see left hind leg) and on the hypoxic regions (see right hind leg). Representative images just after (a and d), 3 days after (b and e), and 13 days after (c and f) initial TOP3 injection are shown.*

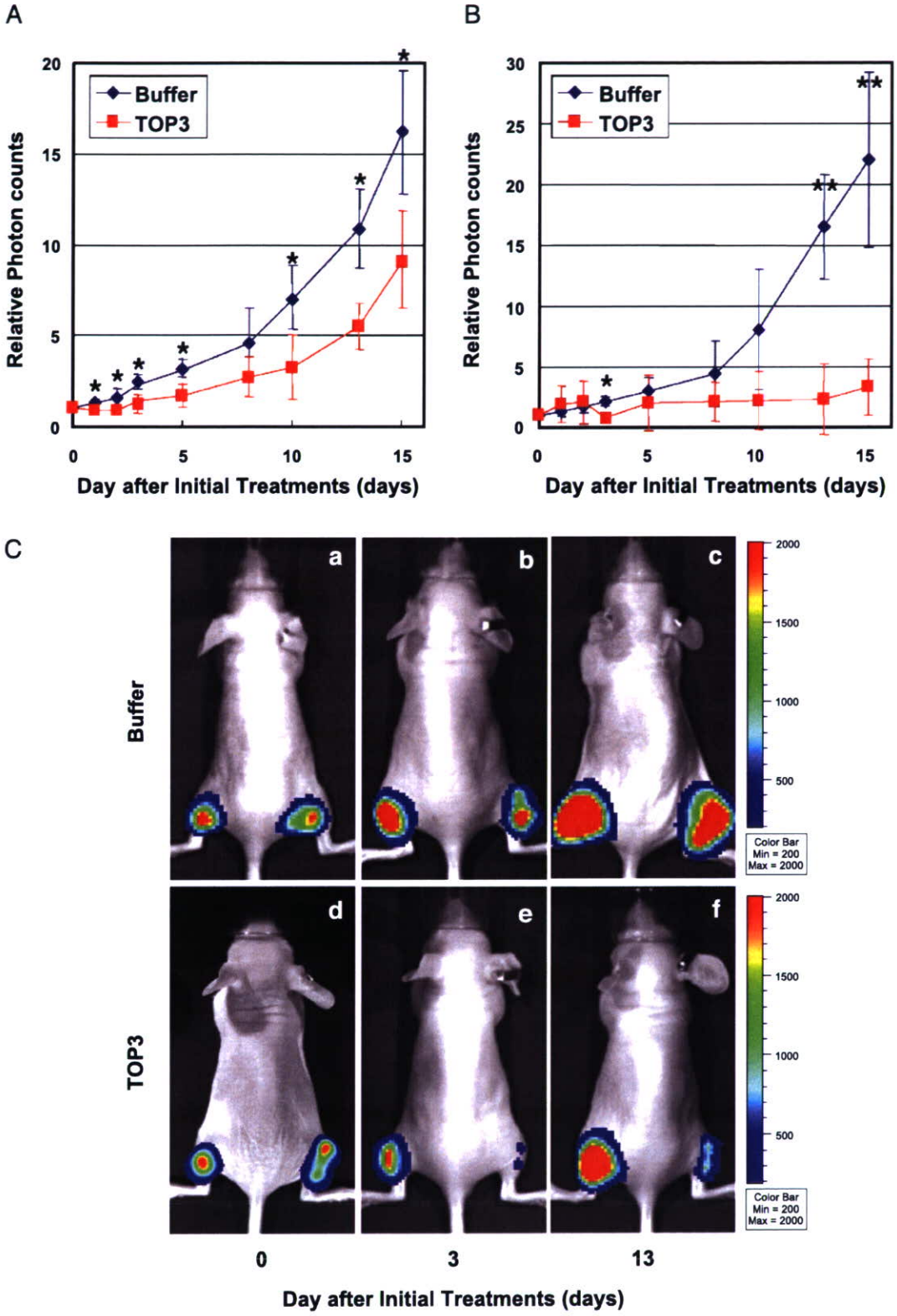
A
B
C
Buffer
TOP3
Relative Photon counts
Day after Initial Treatments (days)
a
b
c
d
e
f
2000
1500
1000
500
Color Bar
Min = 200
Max = 2000
0
3
13

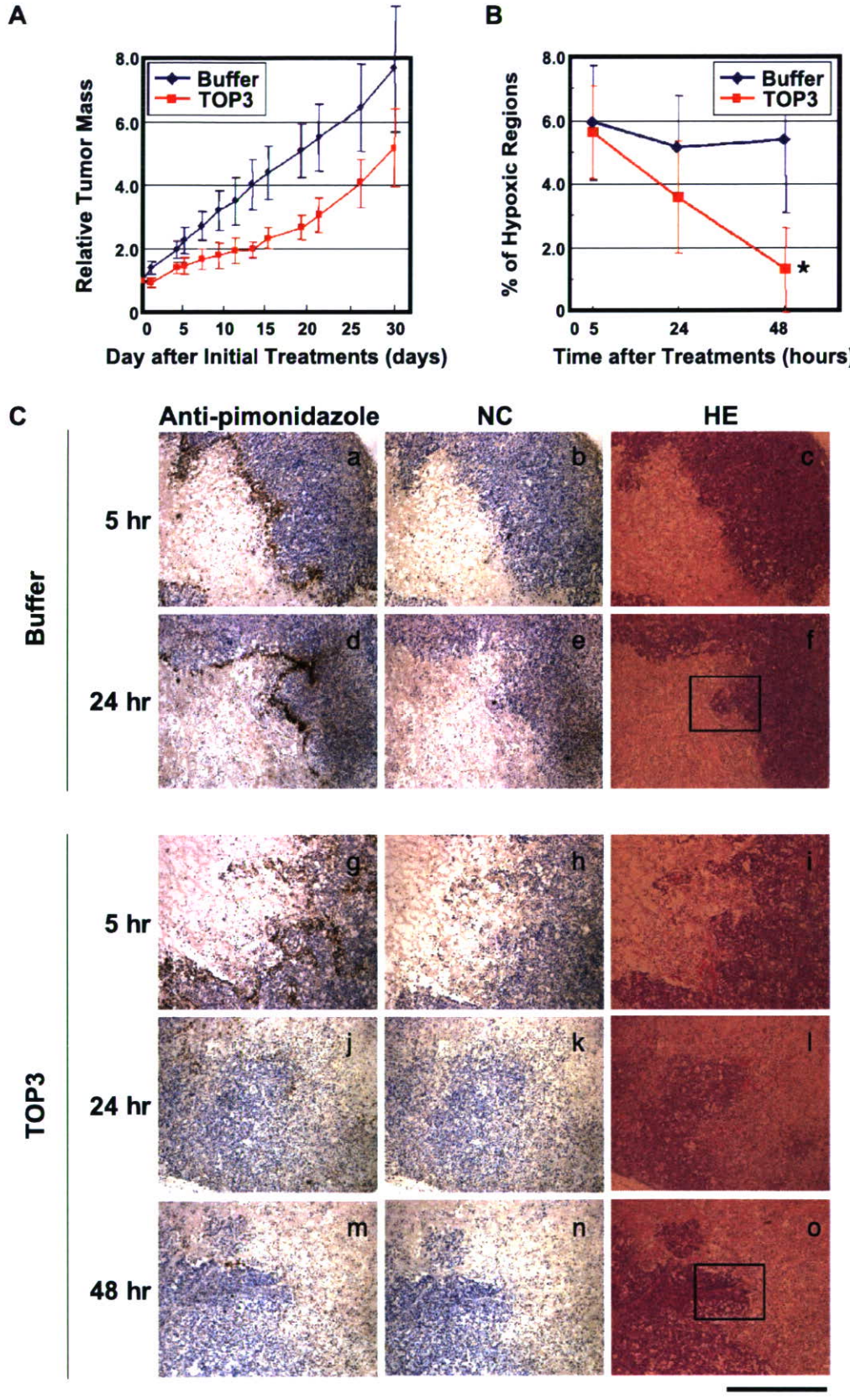
A
Relative Tumor Mass
Buffer
TOP3
8.0
6.0
4.0
2.0
0
0 5 10 15 20 25 30
Day after Initial Treatments (days)
B
% of Hypoxic Regions
Buffer
TOP3
8.0
6.0
4.0
2.0
0
0 5 24 48
*
Time after Treatments (hours)
C
Anti-pimonidazole
NC
HE
Buffer
5 hr
24 hr
TOP3
5 hr
24 hr
48 hr
a
b
c
d
e
f
g
h
i
j
k
l
m
n
o

were totally different from those of buffer-treated ones (Figure 5C). The pimonidazole-positive cells were gradually decreased in the TOP3-treated sections (Figure 5Cg, Cj, and Cm). Higher magnified images clearly show that the boundary areas between viable regions and necrotic regions, which corresponded to pimonidazole-positive cells in buffer-treated xenografts, were empty spaces in the TOP3-treated samples (Figure 6D–F). To investigate the status of the hypoxic tumor cells between 5 and 24 hr after TOP3 treatment, we examined xenografts with TαT-mediated αUTP nick end labelling (TUNEL) at 12 hr after TOP3 treatment. Much more TUNEL-positive green fluorescence was detected around the boundary area between viable and necrotic cells in the TOP3-treated xenograft than in the buffer-treated xenograft (compare Figure 7A with Figure 7D). These data indicate that TOP3 induces apoptosis in hypoxic tumor cells of the boundary regions and efficiently eliminates these cells.

Table 1. Statistical Analysis of TGDT

Treatment	HeLa/5HRE-Luc (days ± SD)	CFPAC-1 (days ± SD)
Buffer	3.2 ± 1.2	4.8 ± 2.3
TOP3	7.6 ± 2.4*	12.6 ± 5.4*

TGDT was calculated as the mean of the days on which relative tumor mass of each tumor reached to two fold of the one on Day 0. Data were based on the results obtained by using HeLa/5HRE-Luc cells (n = 5) and CFPAC-1 cells (n = 6) in Figures 4A and 5A, respectively.
*$p < .05$ (vs. buffer).

Discussion

Recent progress in optical imaging in vivo provides us with various information such as neoplastic cell growth [30], molecular localization [32], enzymatic reaction [33], and protein–protein interactions [34] in living animals. It also contributes towards collecting internal information without the sacrifice of animals. All of the results presented here demonstrate that the optical imaging method using 5HRE-luciferase reporter gene enables us to efficiently and easily monitor tumor hypoxia, where HIF-1 is active in living animals, and precisely evaluate the efficacy of anti-cancer therapies on tumor hypoxia.

HIF-1-dependent promoter has been used to monitor hypoxic status in tumors [20,21,35]. Their reporters were fluorescent proteins. Because permeability of bioluminescence in living animals is much better than fluorescence, a luciferase reporter system allowed sensitive, quantitative, real-time spatio-temporal analyses of the dynamics of neoplastic cell growth [30]. Because the quantitation of total photons from xenografts, in which tumor cells express luciferase gene under a constitutively active promoter, is an indicator of tumor burden [30], progressive tumor growth or regression could be monitored by repeated analyses of HeLa/EF-Luc xenografts at serial time points (Figure 4A and C, tumors in left legs). On the other hand, because the quantitation of total photons from HeLa/5HRE-Luc xenografts is an indicator of tumor hypoxia, qualitative information (hypoxic status) of solid tumors could be obtained by this model system (Figure 4B and C, tumors in right legs). When the growths of HeLa/EF-Luc and HeLa/5HRE-Luc xenografts were assessed with caliper, they were equally suppressed with TOP3 treatment in vivo (data not shown), indicating that both xenografts showed equal sensitivity to TOP3 treatment. These results further strengthen the argument that the decrease in photon counts from TOP3-treated HeLa/5HRE-Luc would reflect the decrease of tumor hypoxia in the xenografts (Figure 4B and C).

According to the previous report, the HIF-1α small interfering (si) RNA, but not the HIF-2α siRNA, suppresses hypoxia-dependent VEGF promoter activity in HeLa cells [36]. This suggests that the HRE from the VEGF promoter is exclusively dependent on HIF-1 activity in HeLa cells. Moreover, Western blot analysis confirmed that the up-regulation of luciferase activity was accompanied with the stabilization of HIF-1α protein in HeLa/5HRE-Luc cells (Figure 1). Because HIF-1 activity is closely associated with tumor hypoxia [37] and the HIF-1-induced expression of luciferase corresponds with hypoxic region in HeLa/5HRE-Luc xenografts (Figure 2A), bioluminescence from the xenografts should reflect the existence of tumor hypoxia where HIF-1 is active.

Figure 5. *Decrease in hypoxic/HIF-1-expressing cells in the TOP3-treated tumor xenografts. (A) CFPAC-1 tumor-bearing mice were intraperitoneally injected with buffer or TOP3 on Days 0, 5, and 10. To calculate the relative tumor mass, the tumor mass measured with caliper on each day was divided by the one on Day 0. Results are the mean of 6 independent tumor-bearing mice ± SD for each group. (B) Tumor xenografts of CFPAC-1 cells were surgically excised 5, 24, or 48 hr after buffer or TOP3 injection, and stained with anti-pimonidazole antibody. To calculate the percentage of hypoxic regions, the percentage of pimonidazole-positive cells to a whole solid tumor was quantified with NIH Image 1.63 software. Results are the mean of three to four tumors from independent tumor-bearing mice ± SD for each group. *$p < .01$. (C) Buffer-treated (a–f) and TOP3-treated (g–o) CFPAC-1 xenografts were surgically excised at the indicated times after the treatments, and serial sections were stained with anti-pimonidazole antibody (a, d, g, j, and m), HE (c, f, i, l, and o), or secondary antibody only as a negative control (NC; b, e, h, k, and n). Three to four tumors from independent tumor-bearing mice were examined for each treatment group and representative tumor sections are shown. Bar = 1 mm. The areas squared in f and o are applied to Figure 6A–C and Figure 6D–6F, respectively.*

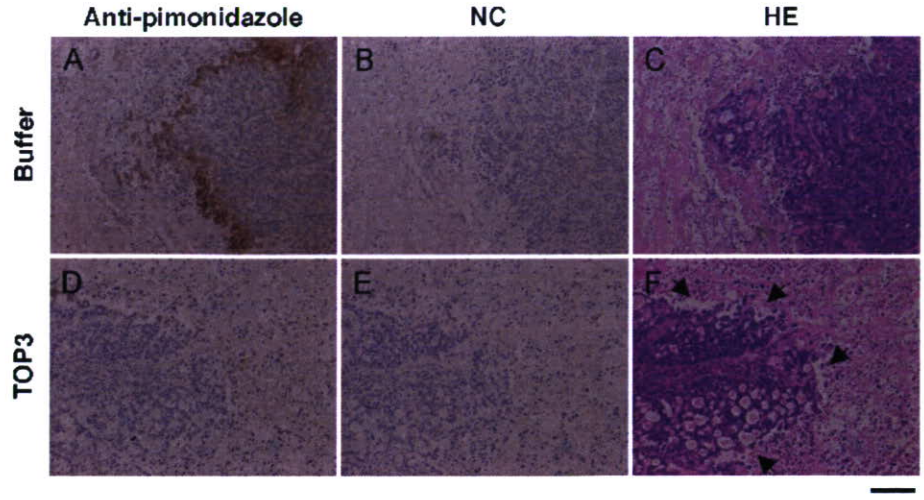

Figure 6. *Effect of TOP3 on hypoxic/HIF-1-expressing cells in xenograft. The areas squared in Figure 5Cf and Co are magnified and shown in A–C and D–F, respectively. Buffer-treated (A–C) and TOP3-treated (D–H) CFPAC-1 xenografts were stained with HE (C and F), anti-pimonidazole antibody (A and D) and without primary antibody as a negative control (NC; B and E). Bar = 100 μm. Arrow = empty spaces between viable region and necrotic region.*

The immunohistochemical analysis using anti-luciferase antibody and anti-pimonidazole antibody indicated that the locations of the luciferase-expressing cells and the pimonidazole-positive cells were very similar. Both of them were located at the boundary areas between viable cells and necrotic regions (Figure 2A). However, their content and intensity were slightly different. The areas where luciferase was expressed were significantly wider than the ones where pimonidazole-positive cells were located. Because the oxygen concentration decreases as the distance from the blood vessels increases, HIF-1α stabilization may have occurred under milder hypoxic conditions than the binding of pimonidazole compounds with thiol groups in proteins, which occurs in less than 10 mmHg [38] (www.radonc.unc.edu/pimo/main.htm). Although oxygen-dependent regulation is the major regulation for HIF-1α expression, we must consider that HIF-1 expression is also affected by oxygen-independent regulation [39,40], and pimonidazole reactivity is absolutely oxygen-dependent [31,38]. Because HIF-1 activity is closely associated with malignant progression [5,16], monitoring HIF-1 activity in solid tumors is crucial for cancer therapy.

Because TOP3 stability is regulated by the same oxygen-dependent mechanism as HIF-1α protein through common ODD domain, both TOP3 and HIF-

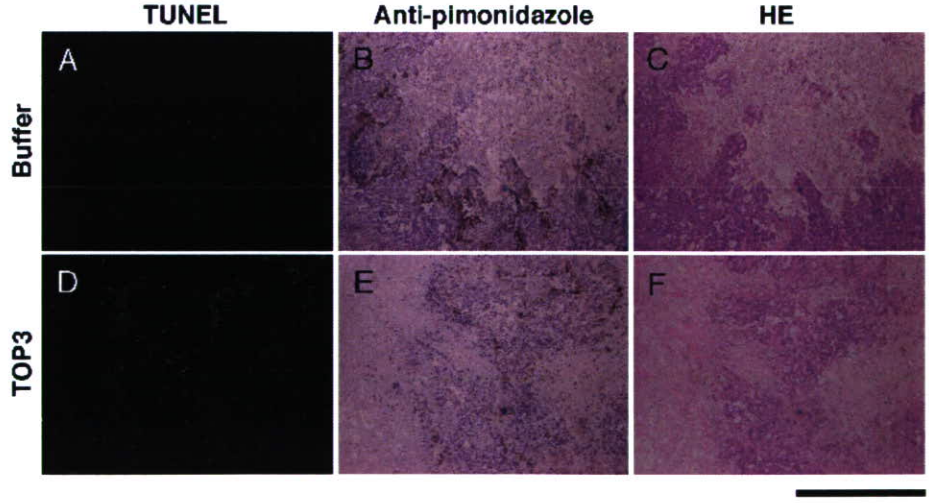

Figure 7. *Apoptosis of hypoxic/HIF-1-expressing cells in TOP3-treated tumor xenograft. CFPAC-1 xenografts excised at 12 hr after either buffer (A–C) or TOP3 (D–F) administration were stained for TUNEL (A and D). Serial tumor sections were stained with anti-pimonidazole antibody (B and E) and HE (C and F). Three tumors were examined for each treatment group and representative tumor sections are shown. Bar = 1 mm.*

1α must be stabilized in the same hypoxic tumor cells in vivo as well as in vitro. Therefore, TOP3 is expected to target HIF-1α-expressing hypoxic tumor cells, leading to shutting off the HIF-1-induced gene expression. In accordance with this expectation, the disappearance of pimonidazole-positive cells from TOP3-treated tumor sections (Figures 5B,C, 6D, and 7E) and the existence of empty spaces between viable and necrotic regions in the TOP3-treated tumor sections (Figure 6D–F) strongly suggests the elimination of hypoxic/HIF-1-expressing cells after TOP3 treatment. Although the disappearance of these areas may be a consequence of the removal of fragile apoptotic cells from the section during the staining process, TOP3-targeted cells must be removed in vivo because the total tumor mass and the photon counts of HeLa/5HRE-Luc xenografts were significantly reduced after TOP3 administration (Figure 4B and C). Although the precise mechanism underlying the removal of hypoxic tumor cells by TOP3 in vivo has not been investigated, it is likely that such cells initially undergo apoptosis, as shown in vitro [23] and in vivo (Figure 7), and that they might be removed by macrophages attracted by the caspase-3-induced "eat-me signal" [41].

TOP3 did not influence luciferase–luciferin reaction in vitro (data not shown). The bioluminescent signals from HeLa/EF-Luc were not so significantly decreased as the one from the HeLa/5HRE-Luc xenografts of TOP3-treated mice (Figure 4C). These results indicate that the significant decrease of the bioluminescent signals from HeLa/5HRE-Luc xenografts of TOP3-treated mice was not simply due to interference of TOP3 in luciferase–luciferin reaction in vivo. Low oxygen concentration influences the luciferin reaction, and thus, we cannot simply compare the bioluminescent signals from HeLa/EF-Luc xenografts with the one from HeLa/5HRE-Luc xenografts. However, as long as monitoring the same HeLa/5HRE-Luc xenografts, the change in the bioluminescent intensity should reflect the amount of hypoxic tumor cells.

The first TOP3 administration caused the most significant reduction in HIF-1 activity on Day 3 (Figure 4B and C). Because HeLa/5HRE-Luc cells had little luciferase activity under aerobic conditions in vitro (Figure 1A), the photon counts detected in the TOP3-treated xenografts on Day 3 may have been background (Figure 4B and Ce). If so, almost all HIF-1-expressing cells were removed as the results of the first administration. The sequential administration with TOP3 in 5-day intervals resulted in remarkable suppression of the increase in the bioluminescence from HeLa/5HRE-Luc xenografts. The relative photon counts from buffer-treated HeLa/5HRE-Luc tumors reached 22-fold, whereas the ones from TOP3-treated tumors were still suppressed on Day 15 (Figure 4B and C). All of these results strongly suggest that the optical imaging of HIF-1 activity by a luciferase reporter system can contribute to the screening and the development of HIF-1-targeting drugs and the convenient evaluation of the efficacy of anti-cancer therapy on tumor hypoxia.

In optical imaging, there was a time lag between the decrease in the photon counts and the elimination of the pimonidazole-positive cells after TOP3 treatment (Figures 4A–C, 5B and C). Concretely, after the first TOP3 administration on Day 0, the tumor became the smallest on Day 2 (Figure 4A) and the pimonidazole-positive cells decreased within 2 days (48 hr; Figure 5B and C), whereas relative photon counts became the lowest on Day 3 (Figure 4B and C). Although luciferase expression is initiated by a hypoxic stimulus, luciferase activity remains even after the surrounding conditions change to aerobic until the protein is degraded. Hence, monitoring the HIF-1 activity as a luciferase activity may not be always punctual. Therefore, it is necessary to further improve the reporter system to realize real-time imaging.

Acknowledgments

We thank Dr. S. Kimura (Kyoto University, Kyoto, Japan) and S. Watanabe (SC BioScience) for IVIS technical support; N. Murakami-Harada, E. Nishimoto, and A. Morinibu for skilled technical assistance. This work was supported by research grants from the Ministry of Education, Science, Sports, and Culture of Japan and Kyoto City Collaboration of Regional Entities for the Advancement of Technological Excellence, JST.

References

[1] Vaupel P, Kallinowski F, Okunieff P (1989). Blood flow, oxygen and nutrient supply, and metabolic microenvironment of human tumors: A review. *Cancer Res.* **49**:6449–6465.

[2] Brown JM (2000). Exploiting the hypoxic cancer cell: Mechanisms and therapeutic strategies. *Mol Med Today.* **6**:157–162.

[3] Teicher BA (1994). Hypoxia and drug resistance. *Cancer Metastasis Rev.* **13**:139–168.

[4] Hockel M, Vaupel P (2001). Tumor hypoxia: Definitions and current clinical, biologic, and molecular aspects. *J Natl Cancer Inst.* **93**:266–276.

[5] Harris AL (2002). Hypoxia—a key regulatory factor in tumour growth. *Nat Rev Cancer.* **2**:38–47.

[6] Hockel M, Schlenger K, Aral B, Mitze M, Schaffer U, Vaupel P (1996). Association between tumor hypoxia and malignant progression in advanced cancer of the uterine cervix. *Cancer Res.* **56**:4509–4515.

[7] Giaccia AJ (1996). Hypoxic stress proteins: Survival of the fittest. *Semin Radiat Oncol.* **6**:46–58.

[8] O'Rourke JF, Dachs GU, Gleadle JM, Maxwell PH, Pugh CW, Stratford IJ, Wood SM, Ratcliffe PJ (1997). Hypoxia response elements. *Oncol Res.* **9**:327–332.

[9] Wang GL, Jiang BH, Rue EA, Semenza GL (1995). Hypoxia-inducible factor 1 is a basic-helix–loop–helix–PAS heterodimer regulated by cellular O_2 tension. *Proc Natl Acad Sci USA.* **92**: 5510–5514.

[10] Bruick RK, McKnight SL (2001). A conserved family of prolyl-4-hydroxylases that modify HIF. *Science.* **294**:1337–1340.

[11] Epstein AC, Gleadle JM, McNeill LA, Hewitson KS, O'Rourke J, Mole DR, Mukherji M, Metzen E, Wilson MI, Dhanda A, Tian YM, Masson N, Hamilton DL, Jaakkola P, Barstead R, Hodgkin J, Maxwell PH, Pugh CW, Schofield CJ, Ratcliffe PJ (2001). C. elegans EGL-9 and mammalian homologs define a family of dioxygenases that regulate HIF by prolyl hydroxylation. *Cell.* **107**:43–54.

[12] Cockman ME, Masson N, Mole DR, Jaakkola P, Chang GW, Clifford SC, Maher ER, Pugh CW, Ratcliffe PJ, Maxwell PH (2000). Hypoxia inducible factor-alpha binding and ubiquitylation by the von Hippel–Lindau tumor suppressor protein. *J Biol Chem.* **275**:25733–25741.

[13] Ohh M, Park CW, Ivan M, Hoffman MA, Kim TY, Huang LE, Pavletich N, Chau V, Kaelin WG (2000). Ubiquitination of hypoxia-inducible factor requires direct binding to the beta-domain of the von Hippel–Lindau protein. *Nat Cell Biol.* **2**:423–427.

[14] Kamura T, Sato S, Iwai K, Czyzyk-Krzeska M, Conaway RC, Conaway JW (2000). Activation of HIF1alpha ubiquitination by a reconstituted von Hippel–Lindau (VHL) tumor suppressor complex. *Proc Natl Acad Sci USA.* **97**:10430–10435.

[15] Tanimoto K, Makino Y, Pereira T, Poellinger L (2000). Mechanism of regulation of the hypoxia-inducible factor-1 alpha by the von Hippel–Lindau tumor suppressor protein. *EMBO J.* **19**: 4298–4309.

[16] Semenza GL (2003). Targeting HIF-1 for cancer therapy. *Nat Rev Cancer.* **3**:721–732.

[17] Hernandez-Alcoceba R, Pihalja M, Qian D, Clarke MF (2002). New oncolytic adenoviruses with hypoxia- and estrogen receptor-regulated replication. *Hum Gene Ther.* **13**:1737–1750.

[18] Kaliberov SA, Buchsbaum DJ, Gillespie GY, Curiel DT, Arafat WO, Carpenter M, Stackhouse MA (2002). Adenovirus-mediated transfer of BAX driven by the vascular endothelial growth factor promoter induces apoptosis in lung cancer cells. *Mol Ther.* **6**: 190–198.

[19] Shibata T, Giaccia AJ, Brown JM (2000). Development of a hypoxia-responsive vector for tumor-specific gene therapy. *Gene Ther.* **7**:493–498.

[20] Vordermark D, Shibata T, Brown JM (2001). Green fluorescent protein is a suitable reporter of tumor hypoxia despite an oxygen requirement for chromophore formation. *Neoplasia.* **3**:527–534.

[21] Liu J, Qu R, Ogura M, Shibata T, Harada H, Hiraoka M (2005). Real-time imaging of hypoxia-inducible factor-1 activity in tumor xenografts. *J Radiat Res (Tokyo).*

[22] Shibata T, Giaccia AJ, Brown JM (2002). Hypoxia-inducible regulation of a prodrug-activating enzyme for tumor-specific gene therapy. *Neoplasia.* **4**:40–48.

[23] Harada H, Hiraoka M, Kizaka-Kondoh S (2002). Antitumor effect of TAT-oxygen-dependent degradation-caspase-3 fusion protein specifically stabilized and activated in hypoxic tumor cells. *Cancer Res.* **62**:2013–2018.

[24] Kizaka-Kondoh S, Inoue M, Harada H, Hiraoka M (2003). Tumor hypoxia: A target for selective cancer therapy. *Cancer Sci.* **94**: 1021–1028.

[25] Schwarze SR, Ho A, Vocero-Akbani A, Dowdy SF (1999). In vivo protein transduction: Delivery of a biologically active protein into the mouse. *Science.* **285**:1569–1572.

[26] Wadia JS, Dowdy SF (2005). Transmembrane delivery of protein and peptide drugs by TAT-mediated transduction in the treatment of cancer. *Adv Drug Deliv Rev.* **57**:579–596.

[27] Inoue M, Mukai M, Hamanaka Y, Tatsuta M, Hiraoka M, Kizaka-Kondoh S (2004). Targeting hypoxic cancer cells with a protein prodrug is effective in experimental malignant ascites. *Int J Oncol.* **25**:713–720.

[28] Kim DW, Uetsuki T, Kaziro Y, Yamaguchi N, Sugano S (1990). Use of the human elongation factor 1 alpha promoter as a versatile and efficient expression system. *Gene.* **91**:217–223.

[29] Sunohara T, Jojima K, Tagami H, Inada T, Aiba H (2004). Ribosome stalling during translation elongation induces cleavage of mRNA being translated in Escherichia coli. *J Biol Chem.* **279**:15368–15375.

[30] Sweeney TJ, Mailander V, Tucker AA, Olomu AB, Zhang W, Cao Y, Negrin RS, Contag CH. (1999). Visualizing the kinetics of tumor-cell clearance in living animals. *Proc Natl Acad Sci USA.* **96**:12044–12049.

[31] Varia MA, Calkins-Adams DP, Rinker LH, Kennedy AS, Novotny DB, Fowler WC Jr., Raleigh JA (1998). Pimonidazole: A novel hypoxia marker for complementary study of tumor hypoxia and cell proliferation in cervical carcinoma. *Gynecol Oncol.* **71**: 270–277.

[32] Chen WT, Tung CH, Weissleder R (2004). Imaging reactive oxygen species in arthritis. *Mol Imaging.* **3**:159–162.

[33] Luker GD, Pica CM, Song J, Luker KE, Piwnica-Worms D (2003). Imaging 26S proteasome activity and inhibition in living mice. *Nat Med.* **9**:969–973.

[34] Ray P, Pimenta H, Paulmurugan R, Berger F, Phelps ME, Iyer M, Gambhir SS (2002). Noninvasive quantitative imaging of protein–protein interactions in living subjects. *Proc Natl Acad Sci USA.* **99**:3105–3110.

[35] Serganova I, Doubrovin M, Vider J, Ponomarev V, Soghomonyan S, Beresten T, Ageyeva L, Serganov A, Cai S, Balatoni J, Blasberg R, Gelovani J (2004). Molecular imaging of temporal dynamics and spatial heterogeneity of hypoxia-inducible factor-1 signal transduction activity in tumors in living mice. *Cancer Res.* **64**: 6101–6108.

[36] Warnecke C, Zaborowska Z, Kurreck J, Erdmann VA, Frei U, Wiesener M, Eckardt KU (2004). Differentiating the functional role of hypoxia-inducible factor (HIF)-1alpha and HIF-2alpha (EPAS-1) by the use of RNA interference: Erythropoietin is a HIF-2alpha target gene in Hep3B and Kelly cells. *FASEB J.* **18**:1462–1464.

[37] Vaupel P (2004). The role of hypoxia-induced factors in tumor progression. *Oncologist.* **5**:10–17.

[38] Raleigh JA, Koch CJ (1990). Importance of thiols in the reductive binding of 2-nitroimidazoles to macromolecules. *Biochem Pharmacol.* **40**:2457–2464.

[39] Zhong H, Chiles K, Feldser D, Laughner E, Hanrahan C, Georgescu MM, Simons JW, Semenza GL (2000). Modulation of hypoxia-inducible factor 1alpha expression by the epidermal growth factor/phosphatidylinositol 3-kinase/PTEN/AKT/FRAP pathway in human prostate cancer cells: Implications for tumor angiogenesis and therapeutics. *Cancer Res.* **60**:1541–1545.

[40] Krieg M, Haas R, Brauch H, Acker T, Flamme I, Plate KH (2000). Up-regulation of hypoxia-inducible factors HIF-1alpha and HIF-2alpha under normoxic conditions in renal carcinoma cells by von Hippel–Lindau tumor suppressor gene loss of function. *Oncogene.* **19**:5435–5443.

[41] Lauber K, Bohn E, Krober SM, Xiao YJ, Blumenthal SG, Lindemann RK, Marini P, Wiedig C, Zobywalski A, Baksh S, Xu Y, Autenrieth IB, Schulze-Osthoff K, Belka C, Stuhler G, Wesselborg S (2003). Apoptotic cells induce migration of phagocytes via caspase-3-mediated release of a lipid attraction signal. *Cell.* **113**:717–730.

A tumor-specific gene therapy strategy targeting dysregulation of the VHL/HIF pathway in renal cell carcinomas

Masakazu Ogura,[1,3] Toru Shibata,[2,6] Junlin Yi,[1,4] Junye Liu,[1,5] Runjiang Qu,[1,5] Hiroshi Harada[1] and Masahiro Hiraoka[1]

[1]Department of Therapeutic Radiology and Oncology, Kyoto University Graduate School of Medicine, 54 Shogoin Kawahara-cho, Sakyo-ku, Kyoto 606-8507, [2]Department of Radiology, Kinki University School of Medicine, 377-2 Oono-Higashi, Sayama, Osaka 589-8511, [3]Department of Radiology, Tenri Hospital, 200 Mishima-cho, Tenri, Nara 632-8552, Japan; [4]Department of Radiation Oncology, Cancer Hospital, Chinese Academy of Medical Sciences and Peking Union Medical College, Beijing, and [5]Department of Radiation Medicine, The Fourth Military Medical University, 17 Chang Le Xi Road, Xian 710032, China

(Received December 15, 2004/Revised February 28, 2005/Accepted March 2, 2005/Online publication May 16, 2005)

Hypoxia-inducible factors, key transcription factors for hypoxia-dependent gene expression, play important roles in angiogenesis and tumor growth. The VHL protein binds to the α subunit of (HIF-α) for its oxygen-dependent degradation. *VHL* mutations are found frequently in sporadic RCC. Disruption of *VHL* results in an abnormal accumulation of HIF-α, leading to the upregulation of downstream genes such as the vascular endothelial growth factor gene. We constructed a luciferase reporter vector driven by hypoxia-responsive elements (5HRE/luc) and a therapeutic vector expressing a herpes simplex virus thymidine kinase gene (5HRE/tk). In the transient transfection assay using VHL-deficient 786-O cells, constitutive luciferase expression was detected under both aerobic and hypoxic conditions. In contrast, 786-O cells transfected with a wild-type *VHL* showed hypoxia-inducible luciferase activity. In *in vitro* MTS assay, 50% of growth inhibition of 786-O cells stably transfected with 5HRE/tk was achieved with exposure to 0.2 μg/mL of GCV under both aerobic and hypoxic conditions. Xenografts of the stable clone in SCID mice exhibited a marked regression on daily injections of GCV (50 mg/kg) for 10 days. In conclusion, a hypoxia-responsive vector may have therapeutic potential for RCC with *VHL* mutations. (*Cancer Sci* 2005; 96: 288–294)

Hypoxia-inducible factors, known as transcription factors, control the expression of genes that play important roles in angiogenesis and tumor growth.[1–3] HIF are composed of a heterodimer of α and β subunits. The α subunit of HIF (HIF-α) is regulated tightly by oxygen availability, while the β subunit (HIF-1β) is expressed constitutively. Three HIF isoforms (HIF-1α, HIF-2α and HIF-3α) similar in structure and binding capability to HIF-1β have been identified.[3] HIF activate transcription by binding to the HRE, which was originally reported in the 3′ flanking region of the human and mouse *Epo* genes.[4,5] Similar HIF binding sites have been found in regulatory regions of other hypoxia-inducible genes, such as *VEGF*, *EPO* and *GLUT-1*.[6–8]

The molecular mechanisms behind the regulation of HIF have been elucidated by recent studies, and indicate that the VHL protein forms an E3 ligase complex in association with elongin B, elongin C, Cul2 and Rbx1,[9–13] which binds to HIF-α for its oxygen-dependent degradation via the ubiquitin–proteasome pathway.[14–17] Furthermore, binding of VHL to HIF requires the hydroxylation of several proline residues within the oxygen-dependent domain of HIF-α in the presence of oxygen.[18–21]

Mutations of the *VHL* tumor suppressing gene are associated with the development of multiple tumors, including hemangioblastomas in the central nervous system, RCC and pheochromocytomas.[22] In sporadic clear cell RCC, which accounts for 75% of RCC,[23] the *VHL* gene was mutated in 33–57% of cases[24–28] and silenced by hypermethylation in an additional 15–19%.[29,30] Interestingly, most of the *VHL* mutations in RCC were located at a particular site within exon 2 encoding the HIF-binding β domain.[31] Thus, disruption of *VHL* results in a marked increase in HIF-1 and/or HIF-2 activity in non-hypoxic conditions because of the impaired VHL-dependent degradation of HIF-1α or HIF-2α, leading to the upregulated expression of VEGF, GLUT-1 and EPO, as demonstrated by studies using VHL-deficient cell lines,[32,33] and clinical samples of RCC.[34–37] From these findings, we speculated that the dysregulation of HIF-α caused by *VHL* mutation in RCC might be exploited as a potential therapeutic target.

Gene therapy has been used in clinical trials for cancer treatment. One of the current problems with cancer gene therapy is the poor targeting selectivity of vectors, leading to a low efficiency of gene transfer to tumor cells and an increased risk of normal tissue toxicity. A tumor-specific gene therapy targeting aberrant transcriptional control may be a solution because the use of tumor-specific promoters can regulate the expression of therapeutic genes at a specific site or in a particular tumor. Several published studies have shown vector systems targeting hypoxic regions within solid tumors, utilizing HRE derived from mouse phosphoglycerate kinase-1,[38] mouse *VEGF*[39] and *EPO*.[40] In an earlier study, a vector construct using five copies of HRE derived from the human *VEGF* gene promoter ligated to a hCMVmp (5HRE/hCMVmp) conferred a marked increase (over 500-fold) in responsiveness to hypoxia in human fibrosarcoma HT1080 cells.[41] Based on this hypoxia-inducible promoter system, a therapeutic model targeting tumor hypoxia was established using the gene for *Escherichia coli* NTR, a prodrug-activating enzyme.[42] HT1080 cells stably transfected with the 5HRE/hCMVmp-NTR vector showed hypoxic induction of NTR gene expression in correlation with increased sensitivity to *in vitro* exposure to the prodrug, and a growth delay was observed in tumor xenografts of the same stable transfectants treated with both intraperitoneal injection of the prodrug and respiration of hypoxic gas.[42] From these findings and results, we expected the hypoxia-inducible vector to be useful for targeting dysregulation of HIF in VHL-deficient RCC as well. The purpose of this study was to test the therapeutic potential of the hypoxia-inducible vector system for RCC harboring *VHL* mutations.

[6]To whom correspondence should be addressed. E-mail: shibata@rad.med.kindai.ac.jp

Abbreviations: CMV, cytomegalovirus; EPO, erythropoietin; GCV, ganciclovir; GLUT-1, glucose transporter 1; HA, hemagglutinin; hCMVmp, human cytomegalovirus minimal promoter; HIF, hypoxia-inducible factor; HRE, hypoxia-responsive element; HSV, herpes simplex virus; HSVtk, herpes simplex virus thymidine kinase gene; luc, luciferase; NTR, nitroreductase; PBS, phosphate-buffered saline; RCC, renal cell carcinoma; RT-PCR, reverse transcription-polymerase chain reaction; SDS, sodium dodecylsulfate; tk, thymidine kinase; VEGF, vascular endothelial growth factor; VHL, von Hippel-Lindau.

 doi: 10.1111/j.1349-7006.2005.00044.x

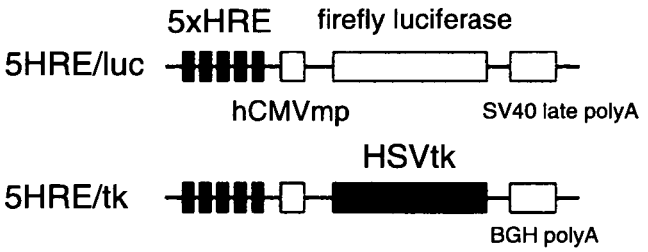

Fig. 1. Structure of hypoxia-inducible plasmids. The constructs of the hypoxia-inducible reporter plasmid 5HRE/luc and the therapeutic plasmid 5HRE/tk are indicated.

Materials and Methods

Hypoxia-inducible vectors. A hypoxia-inducible vector expressing a firefly luciferase gene with a backbone of pGL3 (Promega, Madison, WI, USA) (5HRE/hCMVmp/luc) was constructed previously.[41,43] To generate a 5HRE/tk therapeutic vector, the luciferase gene in the 5HRE/hCMVmp construct with a backbone of pEF/cyto/myc (Invitrogen, Carlsbad, CA, USA) as shown previously,[42] was replaced with a human HSVtk gene (Invivogen, San Diego, CA, USA). Each plasmid construct is shown in Fig. 1.

Cell cultures and hypoxic treatment. Human RCC 786-O cells were purchased from the American Type Culture Collection (Manassas, VA, USA), and 786-O cells stably transfected with either HA-tagged wild-type *VHL* (786-O/VHLwt), HA-tagged truncated *VHL* 1–115 (786-O/VHLmt) or an empty vector (786-O/VHL(–/–)), were provided by Dr Kaelin WG Jr, and are presented as WT8, 115–3, and pRc3, respectively.[44] Untransfected 786-O cells were cultured in Dulbecco's modified Eagle's medium containing 10% fetal bovine serum, while the transfected cells were maintained in the same medium and serum containing 800 μg/mL of G418. Human fibrosarcoma HT1080 cells were maintained in MEMα containing 10% fetal bovine serum. For aerobic incubation, cells were cultured in a well-humidified incubator with 5% CO_2 at 37°C. For hypoxic treatment, cells were cultured in a Bactron II anaerobic environmental chamber (Sheldon Manufacturing, Cornelius, OR, USA) maintained with 90% N_2, 5% H_2 and 5% CO_2.

Transient transfection and luciferase assay. Cells (1×10^5) were seeded in six-well plates 24 h before transfection. Transfection was carried out with 2 μg of 5HRE/luc, 0.04 μg of the control pRL-CMV plasmid (Promega) and 6 μL of Superfect Reagent (Qiagen, Hilden, Germany) according to manufacturer's instructions. The medium was replaced with a fresh batch 3 h after transfection. After incubation for 16–20 h, the cells were trypsinized and split. They were then incubated 10–12 h before either hypoxic or aerobic incubation for 18 h. Cell lysates were then prepared with 400 μL of passive lysis buffer using a Dual luciferase assay kit (Promega). Luciferase activity was measured using a Lumat LB 9507 luminometer (Berthold, Bad Wildbad, Germany).

Immunoblotting analysis. Cells (2×10^5) were seeded in a pair of six-well plates. The next day, one of the plates was kept under hypoxic conditions and the other under aerobic conditions for 18 h. Cells were then collected in 100 μL of 1 × sample buffer (50 mM Tris-HCl [pH 6.8], 100 mM dithiothreitol, 2% SDS, 0.1% bromophenol blue and 10% glycerol) and heated at 95°C for 5 min when 20 μL of each sample was immediately loaded on a SDS polyacrylamide gel (10% for VHL detection; 7.5% for HIF-2α detection) and separated by electrophoresis. To achieve an equal amount of loading between samples, protein volumes were normalized by cell number. Proteins were transferred to a nitrocellulose membrane, blocked with 5% nonfat milk in Tris-buffered saline, and incubated with 0.2 μg/mL of anti-HA antibody (Roche Diagnostics, Indianapolis, IN, USA) for VHL detection or with 0.1 μg/mL of anti-EPAS1 antibody (Santa Cruz Biotechnology, Santa Cruz, CA, USA) for 1 h for HIF-2α detection. Detection was carried out with a chemiluminescence-based method using the ECL Plus Western Blotting Detection System (Amersham Biosciences, Piscataway, NJ, USA).

Stable transfection. To establish stable transfectants of 786-O/VHL(–/–), 786-O/VHLmt, 786-O/VHLwt and HT1080 with the 5HRE/tk vector, 3×10^5 cells were seeded and stably transfected with both 10 μg of 5HRE/tk plasmid and 1 μg of pEF6/Myc-His-A plasmid, which expresses a blasticidin-resistance gene, by a modified calcium-phosphate method. The cells were then trypsinized 24 h after transfection and cultured in the selection medium containing 5 μg/mL blasticidin for 10 days. After selection, the mixtures of each blasticidin-resistant cell were used directly for both RT–PCR analysis and *in vitro* proliferation assay without the isolation as a clone. To establish stable clones of 786-O cells with 5HRE/tk vector, 3×10^5 of 786-O cells were plated in a 6 cm dish. The next day, the cells were transfected with 5 μg of plasmid using 15 μL of Superfect Reagent. They were then trypsinized 24 h after transfection and cultured in the selection medium containing 800 μg/mL of G418. The G418-resistant colonies were isolated and used for *in vitro* cell proliferation assays and mouse xenograft assays.

***In vitro* cell proliferation assay.** One thousand cells were seeded in each well of two 96-well plates and allowed to attach overnight. Cells were treated with medium in the absence or presence of GCV (Invivogen) at various concentrations for 24 h in either hypoxic conditions for 18 h and aerobic conditions for a subsequent 6 h, or else in aerobic conditions for 24 h. The medium was then replaced with fresh medium without the GCV, and subsequent aerobic incubation was carried out for an additional 72 h. Growth inhibition was determined by colorimetric quantification using a Celltiter 96 Aqueous One Solution Cell Proliferation Assay Kit (Promega). Briefly, 10 μL of MTS tetrazonium solution (3-[4,5-dimethylthiazol-2-yl]-5-[3-carboxymethoxyphenyl]-2-[4-sulfophenyl]-2H-tetrazolium, inner salt) was added to each well. After incubation for 2 h, absorbance at 490 nm was measured using a Microplate Reader (Bio-Rad, Hercules, CA, USA). Cell viability was calculated as the ratio of the absorbance value at each condition against that incubated in medium without GCV under continuous aerobic conditions.

Semiquantitative RT–PCR analysis. Blasticidin-resistant stable transfectants of 786-O/VHL(–/–), 786-O/VHLmt, 786-O/VHLwt and HT1080 with 5HRE/tk vector were cultured under aerobic and hypoxic condition for 18 h, and total RNA was extracted using an RNA extraction kit (Qiagen). Complementary DNA was synthesized from 2.5 μg total RNA using an oligo dT-Adaptor Primer (Takara Biomedicals, Tokyo, Japan). Primers used for PCR were HSV/tk-forward: 5′-ATA TCG TCT ACG TAC CCG AG-3′; HSV/tk-reverse: 5′-CGC ACC GTA TTG GCA AGC AG-3′; GAPDH-forward: 5′-ACC ACA GTC CAT GCC ATC AC-3′; and GAPDH-reverse: 5′-TCC ACC ACC CTG TTG CTG TA-3′. The PCR was carried out to amplify the HSV/tk and GAPDH genes for 25 and 20 cycles, respectively. The PCR products were separated by agarose gel electrophoresis and stained with ethidium bromide.

Mouse xenograft assay. Three million cells were suspended in 100 μL PBS and inoculated in the right flank of male 6–8-week-old C.B-17/Icr-*scid* Jcl mice (Clea Japan, Tokyo, Japan). When the tumor volume had reached approximately 200 mm^3, mice were treated daily with 50 mg/kg GCV or a comparable volume of PBS by intraperitoneal injection for 10 days. Tumors were measured using a caliper and tumor volume was calculated

according to the following equation: volume = $0.5 \times a \times b^2$ (a, larger diameter; b, the smaller diameter). The study was approved by the ethical committee of the Kyoto University Institute of Laboratory Animals.

Results

Constitutive luciferase expression of a hypoxia-inducible vector in VHL-deficient and VHL-mutated RCC cells. To test the activity of a hypoxia-inducible vector in VHL-deficient 786-O RCC cells, luciferase activity was examined following transient transfection with a 5HRE/luc vector (Fig. 1). In 786-O/VHL(–/–) cells, strong luciferase expression was detected under both aerobic and hypoxic conditions. This observation was completely different from that for HT1080 cells, as shown in a previous report.[41] We also tested 786-O cells transfected with the wild-type VHLcDNA (786-O/VHLwt), and those transfected with the truncated *VHL* 1–115 (786-O/VHLmt), which is a C-terminal truncation mutant lacking a region frequently altered in sporadic and VHL-related RCC.[44] 786-O/VHLwt showed an inducible luciferase activity in a hypoxia-dependent manner, while 786-O/VHLmt showed a marked expression under both aerobic and hypoxic conditions (Fig. 2A). In addition, we examined the expression of VHL and HIF-2α in an immunoblotting analysis. A protein with the predicted size of the VHL protein was detected in each of 786-O/VHLwt and 786-O/VHLmt. HIF-2α protein was detected under both aerobic and hypoxic conditions in 786-O/VHL(–/–) and 786-O/VHLmt, while hypoxia-dependent HIF-2α expression was detected in 786-O/VHLwt (Fig. 2B), supporting the result of the luciferase assay. Thus, the expression pattern of a hypoxia-inducible vector became constitutive via mutation of the *VHL* gene.

***In vitro* cytotoxicity of 5HRE/tk influenced by different VHL statuses.** To test the therapeutic efficacy, we constructed a plasmid expressing a HSVtk gene based on the same hypoxia-inducible system (Fig. 1). The 5HRE/tk vector was introduced into 786-O/VHL(–/–), 786-O/VHLmt, 786-O/VHLwt and HT1080 cells, and stable transfectants were treated with various concentrations of GCV for 24 h under either 18 h of hypoxic followed by 6 h of aerobic conditions, or continuous aerobic conditions. The growth inhibitory effects were determined by MTS assay 96 h after the start of treatment. In 786-O/VHL(–/–) and 786-O/VHLmt, a growth inhibition rate of 50% was achieved with exposure to less than 0.2 μg/mL GCV under both aerobic and hypoxic conditions. On the other hand, the growth inhibition in both 786-O/VHLwt and HT1080 were observed only under hypoxic conditions, while no significant growth inhibition was observed with exposure up to 10 μg/mL of GCV under aerobic conditions (Fig. 3A). HSVtk transcription levels were examined using semiquantitative RT–PCR analysis (Fig. 3B). High levels of HSVtk transcripts were detected under both aerobic and hypoxic conditions in 786-O/VHL(–/–) and 786-O/VHLmt, but only under hypoxic conditions in 786-O/VHLwt and HT1080 cells, indicating HSVtk transcription levels correlated with sensitivity to GCV. From these results, *in vitro* antitumor effects of 5HRE/tk and GCV gave rise to RCC cells with mutations in the *VHL* gene both under aerobic and hypoxic conditions as well as to hypoxic cells, while cells with wild-type *VHL* were spared under aerobic conditions.

***In vivo* antitumor effects in SCID mouse xenografts of 786-O cells transfected with 5HRE/tk.** To prepare the mouse xenograft model, selected clones of 786-O transfected with 5HRE/tk were established and screened by MTS assay. Among the transfected clones, clone 9 was used for further analysis, indicating a growth inhibition rate of 50% with exposure to less than 0.1 μg/mL GCV under both aerobic and hypoxic conditions (Fig. 4A). On the other hand, the growth of untransfected 786-O cells was not inhibited by up to 10 μg/mL of GCV regardless of hypoxic treatment

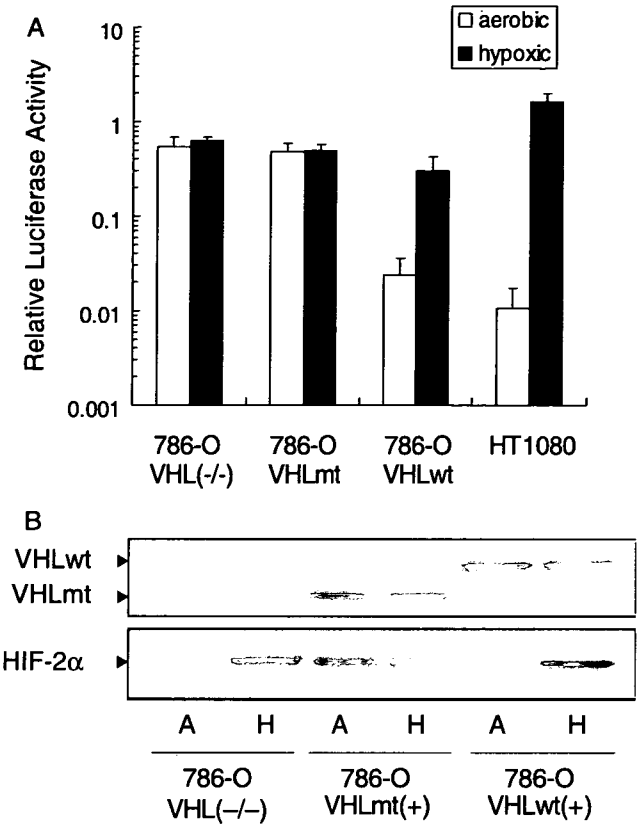

Fig. 2. Constitutive gene expression from the hypoxia-inducible promoter in VHL-deficient and VHL-mutated 786-O cells. (A) Dual luciferase assay was carried out using 786-O/VHL(–/–), 786-O/VHLmt, 786-O/VHLwt and HT1080. The cells were transiently transfected with both 5HRE/luc vector and pRL-CMV, and cultured under aerobic (open bar) or hypoxic (closed bar) conditions. To normalize the firefly luciferase activity from the 5HRE/luc vector, renilla luciferase activity from pRL-CMV was used as an internal control. The normalized luciferase activity under hypoxic conditions was divided by the one under aerobic conditions to calculate the relative luciferase activity. Results are the mean of three independent experiments ± SD. (B) Immunoblots against VHL (upper) and HIF-2α (lower) were carried out using 786-O/VHL(–/–), 786-O/VHLmt and 786-O/VHLwt cells under aerobic (A) and hypoxic (H) conditions.

(Fig. 4A). To confirm *in vivo* therapeutic efficacy, a growth delay assay was carried out. Tumor-bearing mice were treated with daily injections of GCV (50 mg/kg) or PBS for 10 days. In mice with xenografts of clone 9, marked tumor regression was observed during GCV treatment, while tumors treated with PBS continued to grow (Fig. 4B). Among the six mice treated with GCV, three mice showed tumor regrowth after cessation of GCV, while three mice showed stable tumor size (Fig. 4C). On the other hand, the tumor xenografts of untransfected 786-O cells grew regardless of GCV treatment (Fig. 4B).

Discussion

The most common type of human kidney tumors, clear cell RCC, often have mutations of the *VHL* gene, resulting in an abnormal accumulation of HIF-α and upregulation of hypoxia-dependent gene expression driven by HRE regardless of oxygen status. We have developed a hypoxia-inducible vector using HRE derived from human *VEGF* to target hypoxic cells existing in solid tumors and to overcome the resistance of hypoxic cells

 doi: 10.1111/j.1349-7006.2005.00044.x

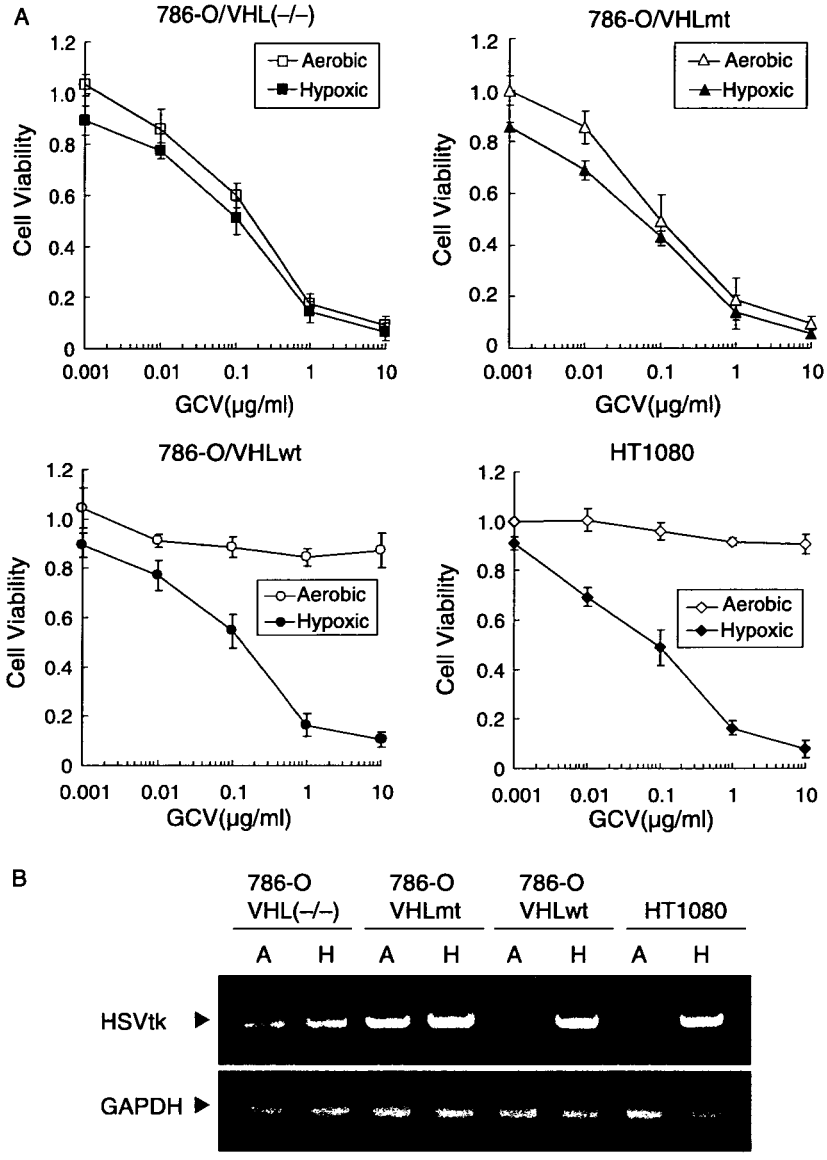

Fig. 3. Cytotoxicity of 5HRE/tk and GCV in VHL(-/-) and VHLmt cells. (A) 786-O/VHL(-/-), 786-O/VHLmt, 786-O/VHLwt and HT1080 were exposed to GCV under aerobic (open) or hypoxic (closed) conditions. Cell viability was quantified using the MTS assay at 72 h after the end of the GCV treatment, and calculated as the ratio of the absorbance value at each condition against that incubated in medium without GCV under continuous aerobic conditions. Results are the mean of three independent experiments ± SD. (B) Cells were cultured under aerobic (A) or hypoxic (H) conditions, and expression of HSVtk mRNA was assessed using semiquantitative RT-PCR using a specific primer set. GAPDH mRNA was also analyzed as an internal control.

to chemotherapy and radiotherapy. Here, we demonstrated a therapeutic model for VHL-deficient RCC using the hypoxia-inducible vector system.

First, we confirmed that HIF transcriptional activity is dysregulated by *VHL* mutations. Luciferase activity was remarkably increased in response to hypoxia in HT1080 and 786-O/VHLwt cells transfected with the 5HRE/luc vector. In 786-O/VHL(-/-) and 786-O/VHLmt, however, strong luciferase expression was detected under both aerobic and hypoxic conditions (Fig. 2A). Figure 2B shows that such dysregulation in 786-O cells is presumably mediated by constitutive HIF-2α expression, because 786-O cells lack HIF-1α.[45] These results are consistent with reports by Maxwell *et al.* and Hu *et al.*[45,46]

HSVtk is a common prodrug-activating gene used in preclinical and clinical trials. GCV is phosphorylated specifically by HSVtk to its monophosphate, which is subsequently converted to the di- and tri-phosphate forms by guanylate kinase and other cellular kinases. GCV-triphosphate can be incorporated into elongating DNA, causing inhibition of DNA replication and single strand breaks.[47] In this study, we constructed HSVtk in conjunction with the 5HRE/hCMVmp promoter as a therapeutic vector. HT1080 and 786-O/VHLwt stably transfected with 5HRE/tk showed that hypoxia-inducible transcription of HSVtk correlated with increased sensitivity to GCV, as had been demonstrated by Shibata *et al.* using the same promoter system.[42] Here, 786-O/VHL(-/-) and 786-O/VHLmt with the 5HRE/tk vector showed hypersensitivity to GCV, together with constitutive HSVtk transcription under both aerobic and hypoxic conditions. From these results, our hypoxia-inducible vector has a selective therapeutic effect not only on hypoxic cells but also on RCC with *VHL* mutations.

According to the mechanism in action described above, the HSVtk–GCV system is particularly suitable for eradication of rapidly dividing tumor cells. On the other hand, because activated GCV is an S-phase-specific cytotoxin, it is necessary that target cells must be actively dividing in S-phase at the time of exposure.[47] As shown in Fig. 4B, xenografts of 786-O cells transfected with 5HRE/tk showed a marked response to GCV and

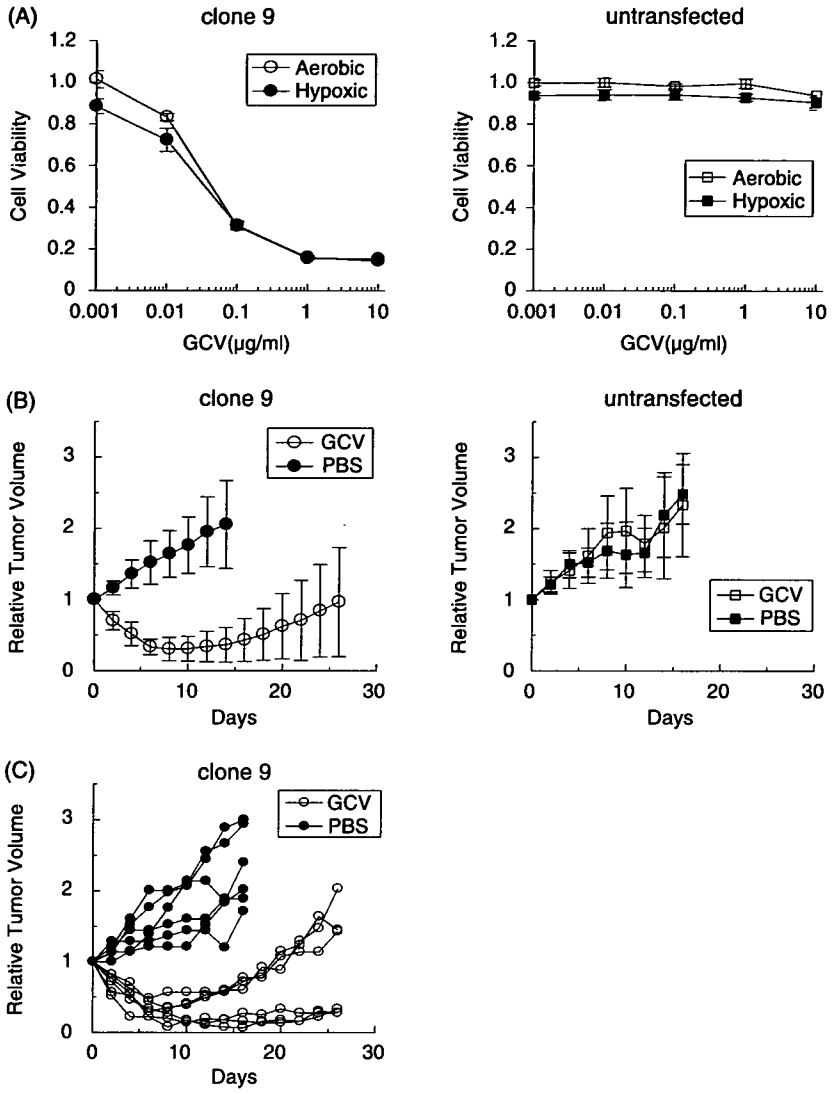

Fig. 4. *In vivo* antitumor efficacy in tumor xenografts consisting of 786-O clone stably transfected with 5HRE/tk. (A) MTS assay was carried out with the stable 786-O clone 9 transfected with 5HRE/tk (left) and untransfected 786-O cells (right), indicating hypersensitivity to GCV in clone 9 under both aerobic (open) and hypoxic (close) conditions. (B) A growth delay assay was carried out using xenografts derived from clone 9 (left) and untransfected 786-O cells (right). Tumor-bearing SCID mice were treated by daily intraperitoneal injection of either 50 mg/kg GCV (open) or a comparable volume of PBS (closed) for 10 days. Relative tumor volume as a function of days from the start of treatment is indicated. Each point and error bar is the mean ($n = 4–6$) and SD. (C) Individual tumor growth derived from clone 9 is indicated.

reduction in size during GCV treatment. However, half of them showed regrowth after cessation of GCV (Fig. 4C). This may be because elimination of activated GCV reactivated division of surviving cells that were not in S-phase during GCV treatment, and because administration dose and/or duration of GCV treatment might have been insufficient to eradicate tumors. In this experimental setting, we did not plan to use 786-O/VHLwt as a control because Iliopoulos *et al.* had already shown that 786-O subclones transfected with the wild-type *VHL* gene suppressed tumor formation in the nude mouse xenograft model.[44]

As shown in Fig. 3A, 786-O/VHLwt and HT1080 transfected with 5HRE/tk exhibited clear differences in sensitivity to GCV under aerobic and hypoxic conditions. These transfectants have no significant growth inhibition with exposure up to 10 μg/mL of GCV under aerobic conditions, suggesting the possibility of the use of the 5HRE promoter to reduce toxicity to normal tissues where hypoxic area dose not usually exist. It would be certain that the use of constitutive promoters such as CMV instead of HRE drive high expression of HSVtk in normal cells that have wild-type *VHL* even under aerobic conditions, which may damage normal cells. *In vivo* toxicity, however, remains to be evaluated with systemic administration of CMV or HRE vectors using a clinically relevant gene delivery system such as viral vectors. Binley *et al.* reported that use of the OBHRE promoter reduced hepatotoxicity with systemic administration of adenoviral vectors.[48]

In this study, we demonstrated the proof-of-principle for a therapeutic model exploiting dysregulation of the VHL/HIF pathway in RCC, providing for the potential application of a hypoxia-inducible vector system to the novel therapeutic treatment of RCC. For clinical application, however, further experiments should be conducted using gene delivery systems such as adenoviral or retroviral vectors, bacteria and macrophages. Of note, a report published during the preparation of this paper demonstrated a therapeutic effect using an oncolytic wild-type adenovirus with HRE from human VEGF gene promote on VHL-deficient RCC.[49]

In present clinical practice, patients with RCC are treated mainly with surgical resection for primary lesions. Metastatic RCC are treated with immunotherapy using interferon-α or interleukin-2, but are still difficult problems. Radiotherapy and chemotherapy are often ineffective. A tumor-specific gene therapy using the hypoxia-responsible vector system may be an option for the treatment of RCC in addition to these therapeutic

 doi: 10.1111/j.1349-7006.2005.00044.x

modalities. Recently, several new therapeutic approaches for RCC have been tested in clinical trials using a radiolabeled chimeric monoclonal antibody targeting CAIX,[50] or using a neutralizing antibody to VEGF.[51]

In conclusion, the hypoxia-inducible vector system may have therapeutic potential for RCC with *VHL* mutations. Further study using delivery systems such as viral vectors, bacteria and macrophages should be conducted for clinical application.

References

1 Semenza GL. HIF-1 and tumor progression: pathophysiology and therapeutics. *Trends Mol Med* 2002; **8**: S62–7.
2 Pugh CW, Ratcliffe PJ. Regulation of angiogenesis by hypoxia: role of the HIF system. *Nat Med* 2003; **9**: 677–84.
3 Safran M, Kaelin WG, Jr. HIF hydroxylation and the mammalian oxygen-sensing pathway. *J Clin Invest* 2003; **111**: 779–83.
4 Semenza GL, Nejfelt MK, Chi SM, Antonarakis SE. Hypoxia-inducible nuclear factors bind to an enhancer element located 3′ to the human erythropoietin gene. *Proc Natl Acad Sci USA* 1991; **88**: 5680–4.
5 Madan A, Curtin PT. A 24-base-pair sequence 3′ to the human erythropoietin gene contains a hypoxia-responsive transcriptional enhancer. *Proc Natl Acad Sci USA* 1993; **90**: 3928–32.
6 Goldberg MA, Schneider TJ. Similarities between the oxygen-sensing mechanisms regulating the expression of vascular endothelial growth factor and erythropoietin. *J Biol Chem* 1994; **269**: 4355–9.
7 Semenza GL, Roth PH, Fang HM, Wang GL. Transcriptional regulation of genes encoding glycolytic enzymes by hypoxia-inducible factor 1. *J Biol Chem* 1994; **269**: 23 757–63.
8 Semenza GL, Jiang BH, Leung SW, Passantino R, Concordet JP, Maire P, Giallongo A. Hypoxia response elements in the aldolase A, enolase 1, and lactate dehydrogenase A gene promoters contain essential binding sites for hypoxia-inducible factor 1. *J Biol Chem* 1996; **271**: 32 529–37.
9 Duan DR, Humphrey JS, Chen DY, Weng Y, Sukegawa J, Lee S, Gnarra JR, Linehan WM, Klausner RD. Characterization of the VHL tumor suppressor gene product: localization, complex formation, and the effect of natural inactivating mutations. *Proc Natl Acad Sci USA* 1995; **92**: 6459–63.
10 Kibel A, Iliopoulos O, DeCaprio JA, Kaelin WG, Jr. Binding of the von Hippel-Lindau tumor suppressor protein to elongin B and C. *Science* 1995; **269**: 1444–6.
11 Pause A, Lee S, Worrell RA, Chen DY, Burgess WH, Linehan WM, Klausner RD. The von Hippel-Lindau tumor-suppressor gene product forms a stable complex with human CUL-2, a member of the Cdc53 family of proteins. *Proc Natl Acad Sci USA* 1997; **94**: 2156–61.
12 Lonergan KM, Iliopoulos O, Ohh M, Kamura T, Conaway RC, Conaway JW, Kaelin WG, Jr. Regulation of hypoxia-inducible mRNAs by the von Hippel-Lindau tumor suppressor protein requires binding to complexes containing elongins B/C and Cul2. *Mol Cell Biol* 1998; **18**: 732–41.
13 Kamura T, Koepp DM, Conrad MN, Skowyra D, Moreland RJ, Iliopoulos O, Lane WS, Kaelin WG Jr, Elledge SJ, Conaway RC, Harper JW, Conaway JW. Rbx1, a component of the VHL tumor suppressor complex and SCF ubiquitin ligase. *Science* 1999; **284**: 657–61.
14 Cockman ME, Masson N, Mole DR, Jaakkola P, Chang GW, Clifford SC, Maher ER, Pugh CW, Ratcliffe PJ, Maxwell PH. Hypoxia inducible factor-alpha binding and ubiquitylation by the von Hippel-Lindau tumor suppressor protein. *J Biol Chem* 2000; **275**: 25 733–41.
15 Kamura T, Sato S, Iwai K, Czyzyk-Krzeska M, Conaway RC, Conaway JW. Activation of HIF1α ubiquitination by a reconstituted von Hippel-Lindau (VHL) tumor suppressor complex. *Proc Natl Acad Sci USA* 2000; **97**: 10 430–5.
16 Ohh M, Park CW, Ivan M, Hoffman MA, Kim TY, Huang LE, Pavletich N, Chau V, Kaelin WG. Ubiquitination of hypoxia-inducible factor requires direct binding to the beta-domain of the von Hippel-Lindau protein. *Nat Cell Biol* 2000; **2**: 423–7.
17 Tanimoto K, Makino Y, Pereira T, Poellinger L. Mechanism of regulation of the hypoxia-inducible factor-1 alpha by the von Hippel-Lindau tumor suppressor protein. *Embo J* 2000; **19**: 4298–309.
18 Hon WC, Wilson MI, Harlos K, Claridge TD, Schofield CJ, Pugh CW, Maxwell PH, Ratcliffe PJ, Stuart DI, Jones EY. Structural basis for the recognition of hydroxyproline in HIF-1 alpha by pVHL. *Nature* 2002; **417**: 975–8.
19 Ivan M, Kondo K, Yang H, Kim W, Valiando J, Ohh M, Salic A, Asara JM, Lane WS, Kaelin WG, Jr. HIFα targeted for VHL-mediated destruction by proline hydroxylation: implications for O_2 sensing. *Science* 2001; **292**: 464–8.
20 Jaakkola P, Mole DR, Tian YM, Wilson MI, Gielbert J, Gaskell SJ, Kriegsheim A, Hebestreit HF, Mukherji M, Schofield CJ, Maxwell PH, Pugh CW, Ratcliffe PJ. Targeting of HIF-α to the von Hippel-Lindau ubiquitylation complex by O_2-regulated prolyl hydroxylation. *Science* 2001; **292**: 468–72.
21 Min JH, Yang H, Ivan M, Gertler F, Kaelin WG Jr, Pavletich NP. Structure of an HIF-1α–pVHL complex: hydroxyproline recognition in signaling. *Science* 2002; **296**: 1886–9.
22 Kim W, Kaelin WG, Jr. The von Hippel-Lindau tumor suppressor protein: new insights into oxygen sensing and cancer. *Curr Opin Genet Dev* 2003; **13**: 55–60.
23 Linehan WM. Molecular targeting of VHL gene pathway in clear cell kidney cancer. *J Urol* 2003; **170**: 593–4.
24 Bailly M, Bain C, Favrot MC, Ozturk M. Somatic mutations of the von Hippel-Lindau (VHL) tumor-suppressor gene in European kidney cancers. *Int J Cancer* 1995; **63**: 660–4.
25 Foster K, Prowse A, van den Berg A, Fleming S, Hulsbeek MM, Crossey PA, Richards FM, Cairns P, Affara NA, Ferguson-Smith MA, *et al.* Somatic mutations of the von Hippel-Lindau disease tumour suppressor gene in non-familial clear cell renal carcinoma. *Hum Mol Genet* 1994; **3**: 2169–73.
26 Gnarra JR, Tory K, Weng Y, Schmidt L, Wei MH, Li H, Latif F, Liu S, Chen F, Duh FM, *et al.* Mutations of the VHL tumour suppressor gene in renal carcinoma. *Nat Genet* 1994; **7**: 85–90.
27 Shuin T, Kondo K, Torigoe S, Kishida T, Kubota Y, Hosaka M, Nagashima Y, Kitamura H, Latif F, Zbar B, *et al.* Frequent somatic mutations and loss of heterozygosity of the von Hippel-Lindau tumor suppressor gene in primary human renal cell carcinomas. *Cancer Res* 1994; **54**: 2852–5.
28 Whaley JM, Naglich J, Gelbert L, Hsia YE, Lamiell JM, Green JS, Collins D, Neumann HP, Laidlaw J, Li FP, *et al.* Germ-line mutations in the von Hippel-Lindau tumor-suppressor gene are similar to somatic von Hippel-Lindau aberrations in sporadic renal cell carcinoma. *Am J Hum Genet* 1994; **55**: 1092–102.
29 Clifford SC, Prowse AH, Affara NA, Buys CH, Maher ER. Inactivation of the von Hippel-Lindau (VHL) tumour suppressor gene and allelic losses at chromosome arm 3p in primary renal cell carcinoma: evidence for a VHL-independent pathway in clear cell renal tumourigenesis. *Genes Chrom Cancer* 1998; **22**: 200–9.
30 Herman JG, Latif F, Weng Y, Lerman MI, Zbar B, Liu S, Samid D, Duan DS, Gnarra JR, Linehan WM, *et al.* Silencing of the VHL tumor-suppressor gene by DNA methylation in renal carcinoma. *Proc Natl Acad Sci USA* 1994; **91**: 9700–4.
31 Brauch H, Weirich G, Brieger J, Glavac D, Rodl H, Eichinger M, Feurer M, Weidt E, Puranakanitstha C, Neuhaus C, Pomer S, Brenner W, Schirmacher P, Storkel S, Rotter M, Masera A, Gugeler N, Decker HJ. VHL alterations in human clear cell renal cell carcinoma. association with advanced tumor stage and a novel hot spot mutation. *Cancer Res* 2000; **60**: 1942–8.
32 Krieg M, Haas R, Brauch H, Acker T, Flamme I, Plate KH. Up-regulation of hypoxia-inducible factors HIF-1α and HIF-2α under normoxic conditions in renal carcinoma cells by von Hippel-Lindau tumor suppressor gene loss of function. *Oncogene* 2000; **19**: 5435–43.
33 Siemeister G, Weindel K, Mohrs K, Barleon B, Martiny-Baron G, Marme D. Reversion of deregulated expression of vascular endothelial growth factor in human renal carcinoma cells by von Hippel-Lindau tumor suppressor protein. *Cancer Res* 1996; **56**: 2299–301.
34 Turner KJ, Moore JW, Jones A, Taylor CF, Cuthbert-Heavens D, Han C, Leek RD, Gatter KC, Maxwell PH, Ratcliffe PJ, Cranston D, Harris AL. Expression of hypoxia-inducible factors in human renal cancer. relationship to angiogenesis and to the von Hippel-Lindau gene mutation. *Cancer Res* 2002; **62**: 2957–61.
35 Wiesener MS, Munchenhagen PM, Berger I, Morgan NV, Roigas J, Schwiertz A, Jurgensen JS, Gruber G, Maxwell PH, Loning SA, Frei U, Maher ER, Grone HJ, Eckardt KU. Constitutive activation of hypoxia-inducible genes related to overexpression of hypoxia-inducible factor-1α in clear cell renal carcinomas. *Cancer Res* 2001; **61**: 5215–22.
36 Igarashi H, Esumi M, Ishida H, Okada K. Vascular endothelial growth factor overexpression is correlated with von Hippel-Lindau tumor suppressor gene inactivation in patients with sporadic renal cell carcinoma. *Cancer* 2002; **95**: 47–53.
37 Na X, Wu G, Ryan CK, Schoen SR, di'Santagnese PA, Messing EM. Overproduction of vascular endothelial growth factor related to von

Acknowledgments

The work was supported in part by Grants-in-Aid for Scientific Research in Priority Areas (12217066) and for Exploratory Research (14657213) from the Japanese Ministry of Education, Culture, Sports, Science and Technology. We thank Dr Kaelin WG Jr for kindly providing the 786-O cell lines stably transfected with different versions of the *VHL* gene. We also thank Akiyo Morinibu for her excellent technical assistance.

Hippel-Lindau tumor suppressor gene mutations and hypoxia-inducible factor-1 alpha expression in renal cell carcinomas. *J Urol* 2003; **170**: 588–92.
38 Dachs GU, Patterson AV, Firth JD, Ratcliffe PJ, Townsend KM, Stratford IJ, Harris AL. Targeting gene expression to hypoxic tumor cells. *Nat Med* 1997; **3**: 515–20.
39 Koshikawa N, Takenaga K, Tagawa M, Sakiyama S. Therapeutic efficacy of the suicide gene driven by the promoter of vascular endothelial growth factor gene against hypoxic tumor cells. *Cancer Res* 2000; **60**: 2936–41.
40 Ruan H, Su H, Hu L, Lamborn KR, Kan YW, Deen DF. A hypoxia-regulated adeno-associated virus vector for cancer-specific gene therapy. *Neoplasia* 2001; **3**: 255–63.
41 Shibata T, Giaccia AJ, Brown JM. Development of a hypoxia-responsive vector for tumor-specific gene therapy. *Gene Ther* 2000; **7**: 493–8.
42 Shibata T, Giaccia AJ, Brown JM. Hypoxia-inducible regulation of a prodrug-activating enzyme for tumor-specific gene therapy. *Neoplasia* 2002; **4**: 40–8.
43 Shibata T, Akiyama N, Noda M, Sasai K, Hiraoka M. Enhancement of gene expression under hypoxic conditions using fragments of the human vascular endothelial growth factor and the erythropoietin genes. *Int J Radiat Oncol Biol Phys* 1998; **42**: 913–16.
44 Iliopoulos O, Kibel A, Gray S, Kaelin WG, Jr. Tumour suppression by the human von Hippel-Lindau gene product. *Nat Med* 1995; **1**: 822–6.
45 Maxwell PH, Wiesener MS, Chang GW, Clifford SC, Vaux EC, Cockman ME, Wykoff CC, Pugh CW, Maher ER, Ratcliffe PJ. The tumour suppressor protein VHL targets hypoxia-inducible factors for oxygen-dependent proteolysis. *Nature* 1999; **399**: 271–5.
46 Hu CJ, Wang LY, Chodosh LA, Keith B, Simon MC. Differential roles of hypoxia-inducible factor 1α (HIF-1α) and HIF-2α in hypoxic gene regulation. *Mol Cell Biol* 2003; **23**: 9361–74.
47 Greco O, Dachs GU. Gene directed enzyme/prodrug therapy of cancer: historical appraisal and future prospectives. *J Cell Physiol* 2001; **187**: 22–36.
48 Binley K, Askham Z, Martin L, Spearman H, Day D, Kingsman S, Naylor S. Hypoxia-mediated tumour targeting. *Gene Ther* 2003; **10**: 540–9.
49 Cuevas Y, Hernandez-Alcoceba R, Aragones J, Naranjo-Suarez S, Castellanos MC, Esteban MA, Martin-Puig S, Landazuri MO, del Peso L. Specific oncolytic effect of a new hypoxia-inducible factor-dependent replicative adenovirus on von Hippel-Lindau-defective renal cell carcinomas. *Cancer Res* 2003; **63**: 6877–84.
50 Divgi CR, Bander NH, Scott AM, O'Donoghue JA, Sgouros G, Welt S, Finn RD, Morrissey F, Capitelli P, Williams JM, Deland D, Nakhre A, Oosterwijk E, Gulec S, Graham MC, Larson SM, Old LJ. Phase I/II radioimmunotherapy trial with iodine-131-labeled monoclonal antibody G250 in metastatic renal cell carcinoma. *Clin Cancer Res* 1998; **4**: 2729–39.
51 Yang JC, Haworth L, Sherry RM, Hwu P, Schwartzentruber DJ, Topalian SL, Steinberg SM, Chen HX, Rosenberg SA. A randomized trial of bevacizumab, an anti-vascular endothelial growth factor antibody, for metastatic renal cancer. *N Engl J Med* 2003; **349**: 427–34.

 doi: 10.1111/j.1349-7006.2005.00044.x